EFFECT OF COMPRESSIBILITY ON THREE-DIMENSIONAL HELICOPTER ROTOR BLADE FLUTTER

A THESIS

Presented to

The Faculty of the Division of

Graduate Studies and Research

By

William Felton White, Jr.

In Partial Fulfillment

of the Requirements for the Degree

Doctor of Philosophy

in the School of Aerospace Engineering

Georgia Institute of Technology

March, 1973

EFFECT OF COMPRESSIBILITY ON THREE-DIMENSIONAL

HELICOPTER ROTOR BLADE FLUTTER

Approved:

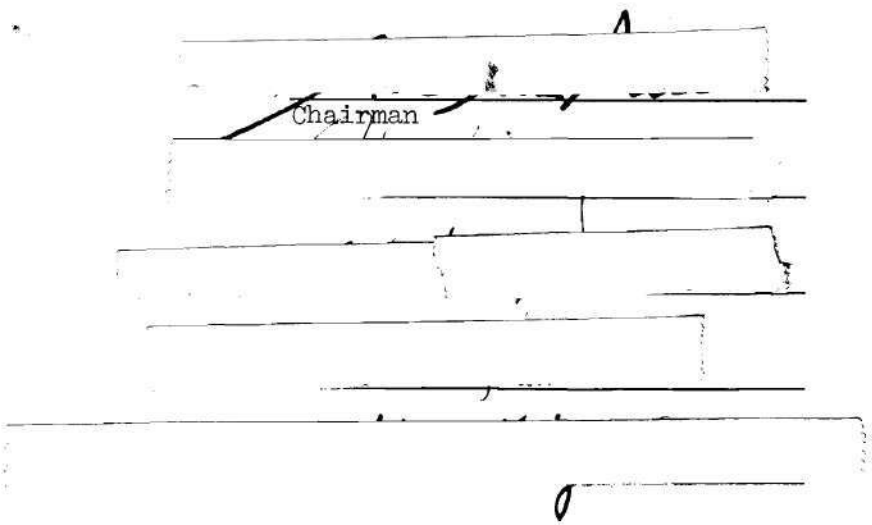

Date approved by Chairman 2·12·73

ACKNOWLEDGMENTS

Acknowledging the many people who have contributed to this thesis is indeed a pleasure. To Dr. G. Alvin Pierce, who suggested the topic and provided most of the wisdom and encouragement necessary for its investigation, I express my deepest appreciation. His guidance throughout my graduate academic career has been invaluable and is appreciated.

Grateful appreciation is extended to Dr. C. V. Smith for his constructive criticism and valuable suggestions for improvement. I would also like to thank the other members of my reading committee, Dr. R. B. Gray, Dr. W. W. King and Dr. M. Stallybrass, for their contributions.

The many discussions with fellow graduate students have provided valuable insight into this and other problems of academic interest. To Dr. Charles E. Hammond and Dr. Felton D. Bartlett, I owe many thanks for their helpful suggestions during the course of this investigation. To Mrs. Ruth Shaw I express my deepest appreciation for her patience and skill in typing the final draft of this thesis.

My wife Martha has contributed most significantly to the successful completion of this thesis and my entire graduate program through her patience, understanding and encouragement. To my parents I owe my entire career. For their many sacrifices during my undergraduate academic program and for impressing upon me the value of knowledge, I express my deepest appreciation.

TABLE OF CONTENTS

		Page
ACKNOWLEDGMENTS		ii
LIST OF TABLES		v
LIST OF ILLUSTRATIONS		vi
NOMENCLATURE		vii
SUMMARY		xi
Chapter		
I.	INTRODUCTION	1
II.	UNSTEADY AERODYNAMIC THEORIES APPLICABLE TO HELICOPTER ROTOR BLADE FLUTTER	5
	Incompressible Theories	
	Compressible Theories	
III.	THEORETICAL DEVELOPMENT	17
	Equations of Motion	
	Flutter Determinant	
	Solution of the Flutter Equations	
IV.	DISCUSSION OF RESULTS	40
	Comparison of Theory with Experiment	
	Evaluation of Computational Efficiency	
V.	CONCLUSIONS AND RECOMMENDATIONS	47
	Conclusions	
	Recommendations	

APPENDIX

A. INTEGRATING-MATRIX METHOD FOR DETERMINING THE COUPLED BENDING-TORSIONAL NATURAL VIBRATION CHARACTERISTICS OF HELICOPTER ROTOR BLADES 49

LITERATURE CITED 79

VITA 82

LIST OF TABLES

Table | Page

1. Comparison of Experimental and Calculated Flutter Speeds 42

LIST OF ILLUSTRATIONS

Figure		Page
1.	Schematic Representation of Unsteady Rotor Flow Field	3
2.	Loewy's Incompressible Aerodynamic Model	6
3.	Flapping Response to Sinusoidal Vertical Hub Displacement as a Function of Frequency Ratio	10
4.	Magnitude of Three Dimensional Lift Distribution Due to Pitching Oscillation of a Single Bladed Rotor About the Quarter Chord Line	12
5.	Compressible Aerodynamic Model for a Multibladed Rotor	14
6.	Variation of the Aerodynamic Coefficients ℓ_α and $\ell_{\dot{\alpha}}$ with Frequency Ratio ($k = 0.10$, $h' = 2.0$)	16
7.	Notation for Blade Displacement	18
8.	Approximation of the Vertical Component of Centrifugal Force	20
9.	Structural Damping Constant for a Model Helicopter Rotor at $M = 0.416$ as a Function of Non-dimensional Tip Speed	43
10.	Structural Damping Constant for a Model Helicopter Rotor at $M = 0.667$ as a Function of Non-dimensional Tip Speed	44

NOMENCLATURE

A_{ij}	element of generalized force matrix defined by Equation (18)
a	elastic axis location (measured in semi-chords from the mid-chord, positive aft)
$\bar{a}$	local lift curve slope
b	blade semi-chord
C	Theodorsen's lift deficiency function
C'	Lowey's modified lift deficiency function
EI	bending rigidity
F'_c	centrifugal force per unit span
F_{ij}	element of flutter determinant defined by Equation (30)
GJ	torsional rigidity
G_i	element of generalized mass matrix defined by Equation (21)
g	structural damping constant
h	non-dimensional vertical deflection of elastic axis (positive down)
h'	non-dimensional vertical distance between successive wake layers
I_α	mass moment of inertia per unit span about the elastic axis
I_1, I_2	mass moment of inertia about major neutral axis and about an axis perpendicular to the chord through the elastic axis
i	imaginary number = $\sqrt{-1}$
k	reduced frequency = $\omega b/\Omega y$

L_α, L_h	unsteady aerodynamic lift coefficients
L'	aerodynamic lift per unit span (positive down)
ℓ_α	unsteady aerodynamic coefficient = $- k^2 \left[\Re\left(L_\alpha\right) - \frac{1}{2} \Re\left(L_h\right) \right]$
$\ell_{\dot{\alpha}}$	unsteady aerodynamic coefficient = $- k \left[\Im\left(L_\alpha\right) - \frac{1}{2} \Im\left(L_h\right) \right]$
M	Mach number or number of normal modes (meaning clear in context)
M'	aerodynamic moment about the elastic axis per unit span (positive nose-up)
M_c'	centrifugal moment about the elastic axis per unit span
M_α, M_h	unsteady aerodynamic moment coefficients
m	mass per unit span
$\bar{m}$	mass per unit area
n	number of spanwise stations used for modal analysis
P	length of blade interval
Q	number of blades in rotor or generalized force (meaning clear in context)
q	blade number
R	blade radius
r	local blade radius
r_α	non-dimensional radius of gyration about the elastic axis
S_α	static unbalance per unit span about the elastic axis
T	kinetic energy or axial tension force in Appendix A
T'	kinetic energy per unit span
t	time

U	vertical velocity of rotor or strain energy
u	inflow velocity (steady, normal to rotor disc)
V	free stream velocity
w	vertical deflection of elastic axis (positive down)
x	coordinate in stream direction along the airfoil (positive aft)
x_α	non-dimensional static unbalance arm
y	coordinate in the spanwise direction (positive outboard)
z	coordinate in the vertical direction (positive up)
α	angle of attack (positive nose up)
α_t	blade twist (steady, positive nose up)
β	blade flapping angle
η	non-dimensional spanwise variable = y/R
θ	local slope of elastic axis (positive clockwise)
λ	complex eigenvalue defined by Equation (31) or dummy variable (meaning clear in context)
μ	mass ratio
ν	frequency ratio = ω/Ω
ξ	generalized coordinate
σ	rotor density parameter = $2bQ/\pi R$
ρ	mass density of air
ϕ	eigenvectors defined by Equation (9)
Ω	rotational speed of rotor
ω	oscillatory frequency
ω_n	undamped natural frequency of the n^{th} mode

Subscripts

c	quantity associated with centrifugal loads
h, z	quantity associated with plunging motion
i	quantity associated with mode shape; denotes function evaluated at a specific spanwise interval where i = 1, 2 . . . n
j	quantity associated with mode shape
M	number of vibration modes
o	quantity at rotor root; standard atmosphere
t	quantity at rotor tip
α	quantity associated with pitching motion
∞	refers to free-stream conditions

Matrix Notation

$[\ ]$	square matrix
$\begin{bmatrix} \ddots & \\ & \ddots \end{bmatrix}$	diagonal matrix
$\{\ \}$	column matrix
$\begin{bmatrix} \cdots \end{bmatrix}$	row matrix
$[\ ]^{-1}$	inverse matrix
$[\ ]^{T}$	transpose matrix
$\begin{bmatrix} 1 & \\ & \ddots \end{bmatrix}$	identity matrix

SUMMARY

An analytical study is presented to determine a flutter criterion applicable to helicopter rotor blades. To accomplish this, it is necessary to establish the relative accuracy and computational efficiency of compressible unsteady aerodynamic theories applicable to rotor blades. Considerations are restricted to the "classical" flutter of an equivalent single bladed rotor in hover at low inflow. Strip theory is used to compute aerodynamic loads. Comparison is made with experimental data.

CHAPTER I

INTRODUCTION

Improvements in modern helicopter technology require consideration of innovative and advanced rotor blade concepts. Design methods have resulted in the evolution of present rotors without adequate definition of aerodynamic and dynamic characteristics.

The most important single component of a flutter analysis is the representation of the aerodynamic loads. Flutter is a well defined phenomenon for fixed wing vehicles whose lifting surfaces experience a uniform free stream velocity at each spanwise station. A helicopter rotor does not experience a uniform velocity at each spanwise station. Therefore, the definition of flutter and an associated flutter boundary must be re-examined.

As fixed wing vehicles have progressed from low subsonic to the hypersonic flight regime, approximate unsteady aerodynamic theories have evolved to assist in predicting and understanding the associated aeroelastic instabilities. In the case of helicopter rotors, a parallel development of appropriate aerodynamic theory is far from complete. A major reason for this deficiency is the extremely complicated flow field of a helicopter rotor.

The vorticity shed from an oscillating lifting surface of a conventional aircraft remains almost in the plane of the lifting surface as it moves downstream. In contrast the vorticity shed from a

helicopter rotor forms a helical pattern below the rotor disk due to the presence of a finite inflow through the disk. In forward flight this helix is skewed in the downstream direction while in vertical ascent or hover it is displaced axially below the plane of the rotor disk. Figure 1 illustrates this helical pattern for the condition of high and low inflow in vertical ascent. In the case of high inflow, illustrated in Figure 1A, the shed vorticity is rapidly displaced below the plane of the rotor. In such cases it is admissible to use fixed wing unsteady aerodynamics in a strip theory fashion provided the spanwise velocity gradient is incorporated. The condition of low inflow shown in Figure 1B yields a radically different vorticity pattern below the rotor disk. The axial displacement of the shed vorticity from previous passages of the rotor and other rotors in the system is significantly less for low inflow. The proximity of the wake vorticity pattern to the rotor precludes the use of fixed-wing unsteady aerodynamic theory. However, practically all published flutter analyses (see References [1],[2],[5], and [6]) have utilized fixed-wing unsteady aerodynamics for both conditions shown in Figure 1. In addition, many investigations were based on quasi-steady aerodynamic derivatives. Most previously published helicopter flutter analyses have placed considerable emphasis on accurately representing the structural dynamic properties of the rotor. As a result of using fixed wing aerodynamics the predicted flutter can be extremely unconservative. Thus, the understanding of the mechanism of aeroelastic flutter of rotors is significantly less than corresponding fixed wings.

The lack of adequate aerodynamic theory has led helicopter

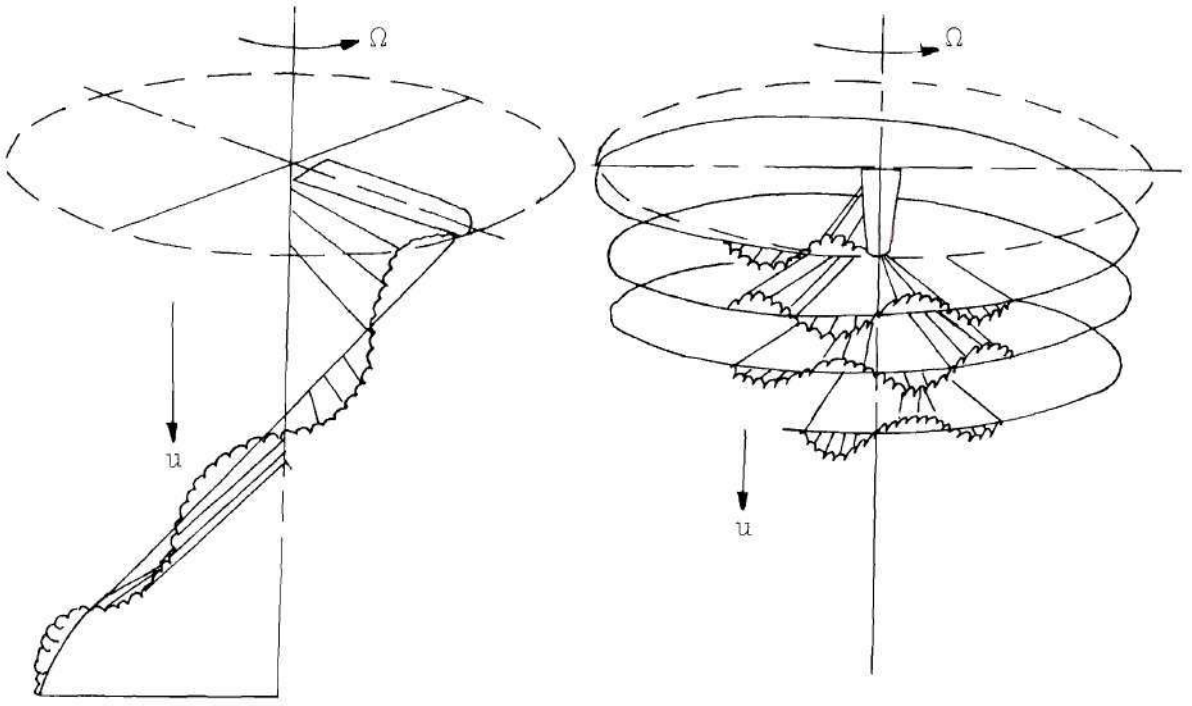

A. High Inflow

B. Low Inflow

Figure 1. Schematic Representation of Unsteady Rotor Flow Field

designers to rely heavily on past experience and fixed wing theory. However, advances in helicopter design by these methods have progressed to the level that their future use is questionable. Recently a limited number of investigations, (see References [7-11]) primarily outside the mainstream of helicopter design, followed the logical method of replacing the rotor and its complicated wake with a simplified but tractable model. Using this simplified model, it was then possible to apply the many proven methods of fixed wing analyses to predict the unsteady aerodynamic loads on a helicopter rotor. However, calculation of the aerodynamic loads is arduous and time consuming due to the enormously complicated effects of the wake.

The analysis of rotor aeroelastic flutter also requires appropriate representation of the structural dynamic characteristics. In general structural dynamic methods used for fixed wings are applicable provided that the centrifugal force is included. However, helicopter rotors exhibit numerous root boundary conditions including feathering, inplane and flapping hinge offsets from the axis of rotation which lead to kinematic coupling. Furthermore, the possibility of rotor hub elasticity must be considered. Numerous satisfactory methods of representing the structural dynamics of a rotor are available (see References [1-6]). These methods approximate a continuous structure possessing infinite degrees of freedom by a discrete system with finite degrees of freedom.

CHAPTER II

UNSTEADY AERODYNAMIC THEORIES APPLICABLE TO HELICOPTER ROTOR BLADE FLUTTER

In this chapter the available unsteady aerodynamic theories applicable to rotor blade flutter are reviewed. Although the emphasis of this research is within the subsonic compressible regime, both incompressible and compressible aerodynamic theories are compared. The incompressible methods provide valuable insight into the complicated flow field of a helicopter rotor. Also physical parameters which are unique to the unsteady aerodynamic theory of helicopter rotors are readily identified.

Incompressible Theories

The first significant development in the unsteady aerodynamic theory of helicopter rotors was made independently by Loewy [7], Jones [8], and Timman and Van de Vooren [9]. In this approach, which considered the flow to be incompressible, various assumptions were introduced to make the mathematical analysis more tractable. The primary restriction is that the helicopter is assumed to be operating in a vertical ascent or hovering condition. Within these restrictions it was possible to reduce the complicated three-dimensional rotor flow field to a more manageable two-dimensional flow field. The resulting two-dimensional mathematical model as illustrated in Figure 2 included

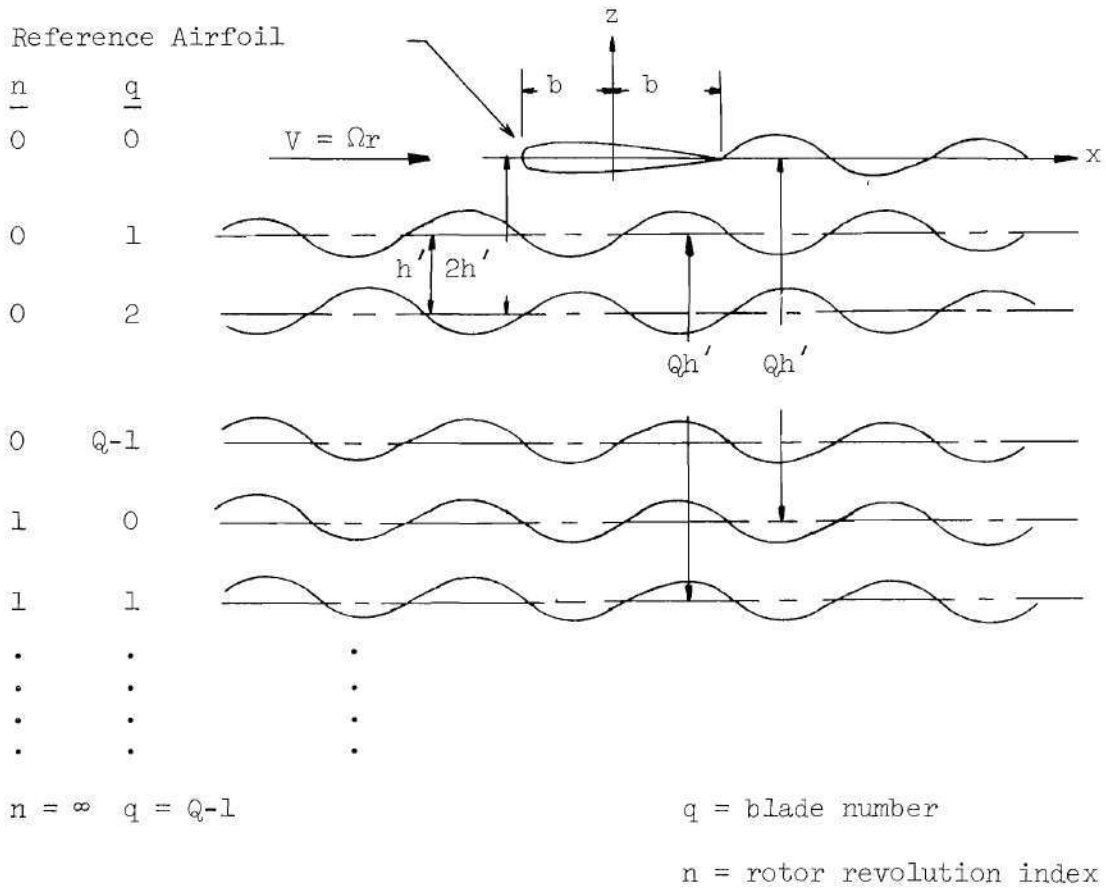

Figure 2. Loewy's Incompressible Aerodynamic Model

a reference airfoil together with a system of wakes shed by the other blades as well as the wake shed by the reference blade during previous revolutions. Using this two-dimension approximation to the rotor flow field Loewy [7] was able to show that the loading on the reference airfoil could be written in the same form as the loading on an oscillating two-dimensional fixed wing airfoil. This fixed wing result was originally given by Theodorsen [10] in terms of a lift deficiency function (Theodorsen function) which modified the quasi-steady circulatory lift. The only difference between the results of Loewy and Theodorsen is that the complex lift deficiency function is modified to account for the layers of vorticity below the reference airfoil. The lift deficiency function from fixed wing theory is a function of only reduced frequency. However, Loewy's modified form is a function of reduced frequency k, frequency ratio ν and inflow ratio h' which determines the wake spacing below the reference airfoil. The significance of Loewy's analysis is the introduction of frequency ratio and inflow ratio as parameters appearing only in the modified lift deficiency function. In addition to the known importance of reduced frequency, both frequency ratio and inflow ratio were shown to be of major importance in determining the unsteady aerodynamic loads of a helicopter rotor.

Using fixed-wing unsteady aerodynamic theory for comparison Loewy found that the aerodynamic coefficients were significantly different for low inflow. For the condition of high inflow, increasing agreement was demonstrated and identical results obtained for infinite wake spacing. At a finite inflow ratio the aerodynamic coefficients

were found to be cyclic in frequency ratio ν. Moreover, it was found that the lift damping derivatives in pitch and translation abruptly decreased in magnitude near integer values of ν and that high inflow attenuated this decrease. In the case of a multiple blade rotor system this behavior occurs near multiple integer values of the number of blades. Thus a two bladed rotor system would experience an abrupt decrease in the magnitude of damping derivatives near even integer values of ν.

The unsteady aerodynamic theory of Loewy was used by Hammond [11] to investigate the flutter characteristics of a two-dimensional section of a rotor. A comprehensive parametric variation established the significance of frequency ratio and inflow ratio on the flutter characteristics of this section. Hammond [11] found that the presence of the wake below the plane of the rotor is a destablizing influence. The frequency ratio ν was shown to be a major importance in determining flutter speed. At near integer values of ν a significant destablizing influence was observed. Thus, Hammond [11] verified Loewey's conclusions that an abrupt decrease of the aerodynamic damping derivatives near integer values of ν could lead to an aeroelastic instability. An important aspect of Hammond's two-dimensional flutter analysis is the apparent similarity between the fixed wing and rotor damping plots. It is obvious that this apparent similarity of damping plots in a two-dimensional rotor flutter analysis is a consequence of ν and k being independent parameters. As discussed later, the damping plots of a finite rotor are significantly influenced by the cyclic behavior of the aerodynamic coefficients.

Experimental verification of the oscillatory behavior of rotor aerodynamic coefficients was provided by Ham, Moser and Zvara [12]. A vibration test of a two-bladed rotor model was conducted by vibrating the hub in an axial direction and observing the resulting response of the elastic rotor. Their results are illustrated in Figure 3 where it is observed that abrupt resonant peaks in the vibratory response, which denotes a loss of aerodynamic damping, occur at even integer values of frequency ratio. They were also able to predict this response using Loewy's modified lift deficiency function, $C'(k,\nu, h')$, while Theodorsen's function, $C(k)$, for fixed wings failed to exhibit this behavior. These experimental results strongly imply that a corresponding abrupt loss of aerodynamic damping would significantly affect the flutter characteristics of helicopter rotors. An extensive review of the literature failed to yield experimental or analytical flutter data exhibiting this phenomenon of abrupt loss of aerodynamic damping.

A limited number of three-dimensional unsteady aerodynamic theories have been published. Miller [13] has presented a summary of the past approaches taken in obtaining rotor blade aerodynamic loads. In this approach the aerodynamic loads resulting from the near wake are treated using lifting surface theories, while the far wake is treated using the lifting line approximation.

Ashley, Moser and Dugundji [14] present a comprehensive unsteady lifting surface theory for a helicopter rotor in hover flight. Reissner's [15] fixed wing unsteady lifting line theory is extended to incorporate the spanwise velocity gradient. The wake shed below

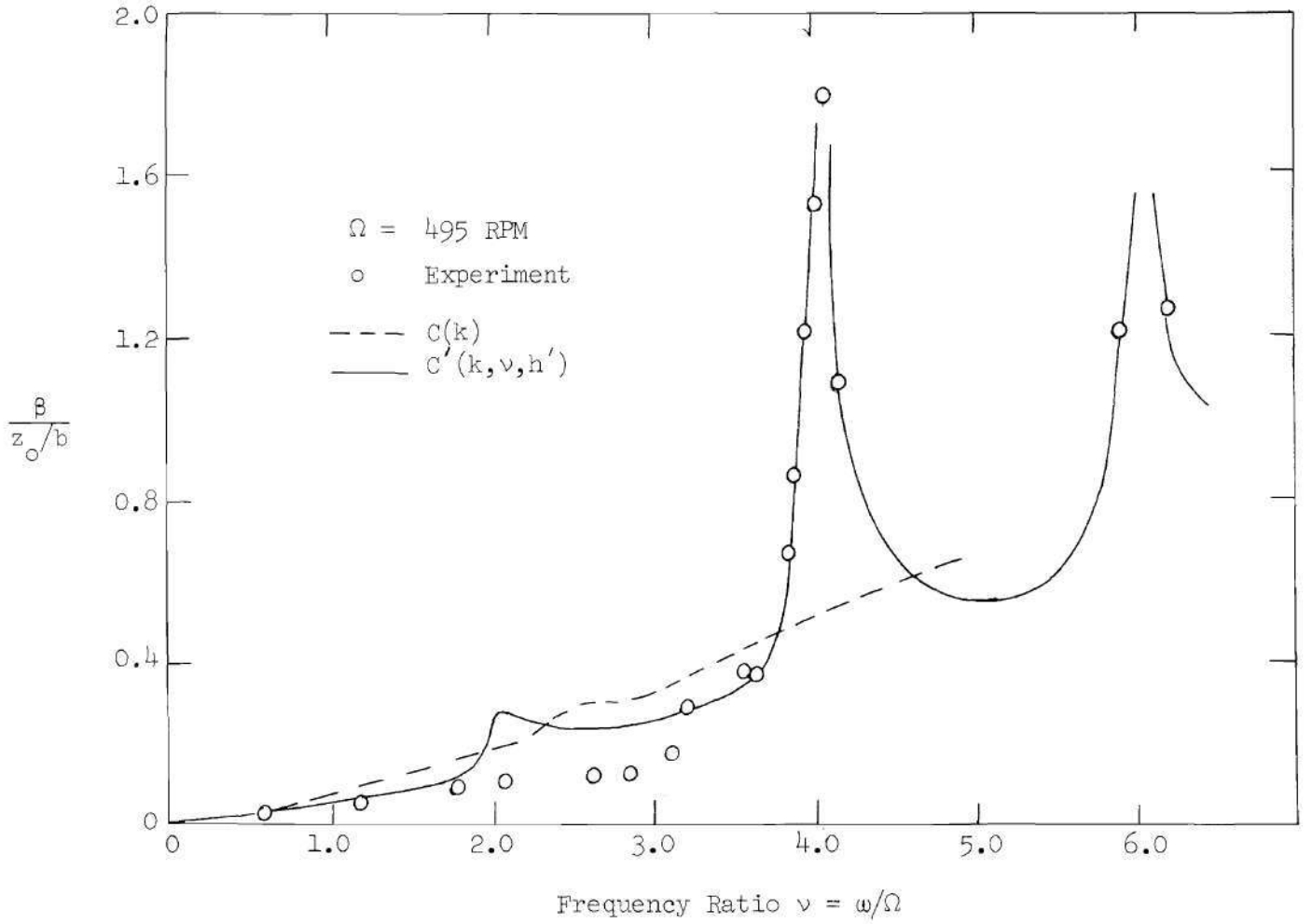

Figure 3. Flapping Response to Sinusoidal Vertical Hub Displacement as a Function of Frequency Ratio

the lifting surface is incorporated by utilizing Loewy's wake model. Aerodynamic loads are computed by combining Reissner's approximations, incorporating the spanwise velocity gradient and replacing $C(k)$ with Loewy's modified lift deficiency function $C'(k,\nu,h')$. Unlike the applicability and mathematical simplicity of Loewy's two-dimensional theory, the analytic development and numerical application of this three-dimensional theory are rather involved and lengthy. The results of representative numerical calculations from Reference [14] provides valuable, if not the only, insight into three-dimensional effects on unsteady aerodynamic loads. Figure 4 shows the magnitude of the three-dimensional lift distribution due to pitching oscillation. The consequence of neglecting the wake is significant for both two-dimensional and three-dimensional calculations. In addition, Figure 4 indicates that differences between two-dimensional and three-dimensional calculations including the wake are negligible except near the tip. Reference [14] concluded that three-dimensional effects, with the exception of small phase shifts, were such that, under some circumstances, strip theory could be applied. These results do not account for the potentially large influence of the strong helical vortices near the tip.

In a recent publication, Ichikawa [16] presents a comprehensive lifting surface theory for a helicopter rotor in forward flight. In this theory, the lifting surface equations are developed for a rotor in forward flight and then a reduction to the lifting line equations is made through approximations equivalent to those of Weissinger's [17] L-method.

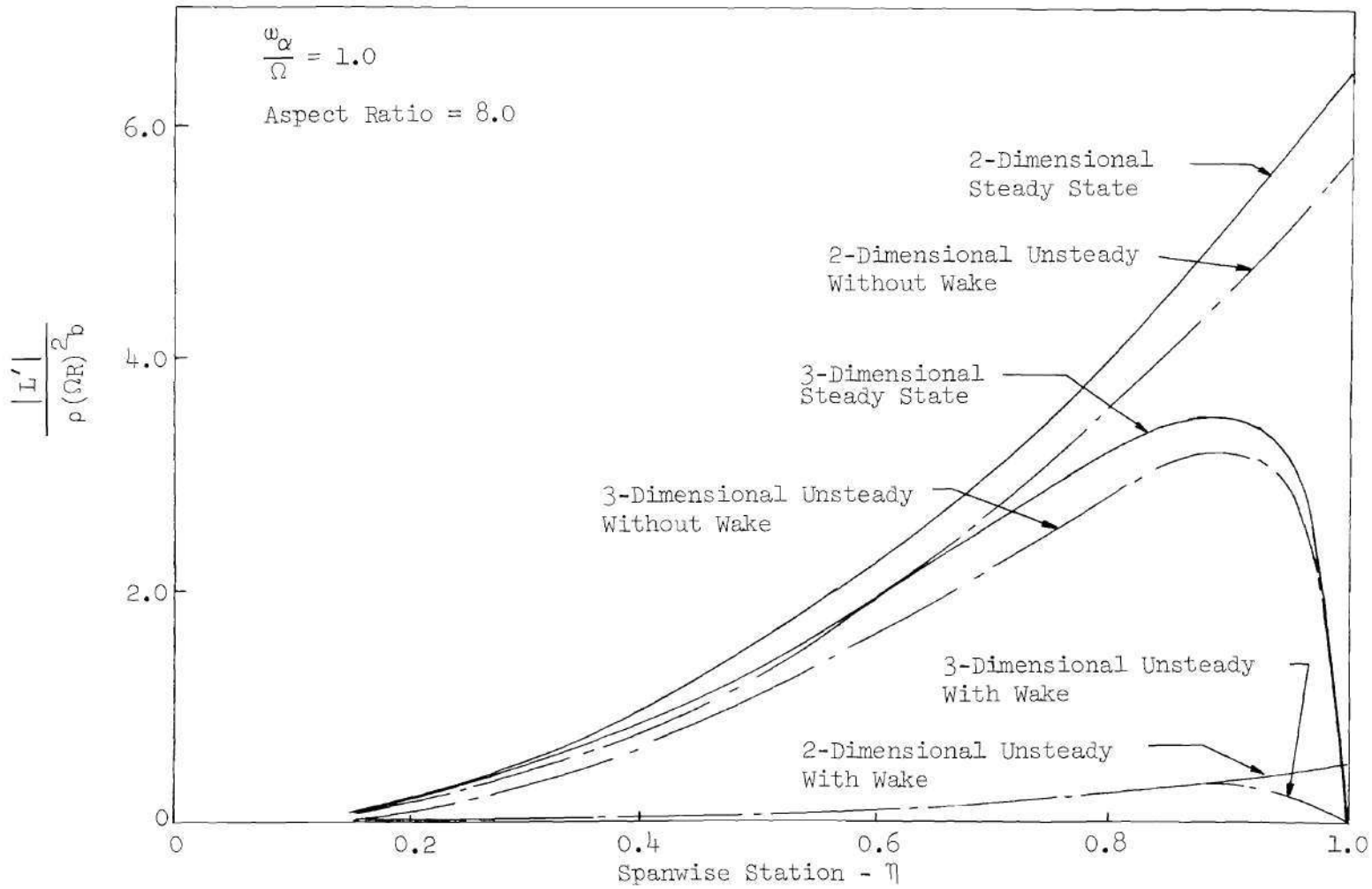

Figure 4. Magnitude of Three Dimensional Lift Distribution Due to Pitching Oscillation of a Single Bladed Rotor About the Quarter Chord Line

In general, the complexity of these unsteady lifting surface theories precludes their use for practical flutter analysis to rapidly obtain estimates of flutter speed and the effect of varying blade parameters on flutter speed. In succinct terms, the required amount of systematization and breadth of applicability is yet to be achieved by three-dimensional unsteady aerodynamic theories.

Compressible Theories

Modern helicopters operate with high tip speeds in the subsonic range, thus indicating that compressibility effects should be included in an analysis of rotor flutter.

The aerodynamic model treated by Loewy as illustrated in Figure 2 was recently analyzed by Jones and Rao [18] to include compressibility effects. Instead of using an incompressible vortex solution, Jones and Rao incorporated a compressible solution for the velocity potential in conjunction with Loewy's flow model. Their analysis follows a technique developed earlier by Jones [19] for the two-dimensional fixed wing oscillating in subsonic flow.

Hammond [20] independently analyzed a slightly different model of the two-dimensional compressible problem. Hammond's mathematical model is shown in Figure 5. The acceleration potential approach which has proved fruitful in fixed wing analysis was used by Hammond. With a velocity potential approach such as used by Jones and Rao, the elemental vorticity must be distributed in the wake and on the airfoil to account for the velocity discontinuity across the wake and airfoil. In contrast, however, the acceleration potential used by Hammond is

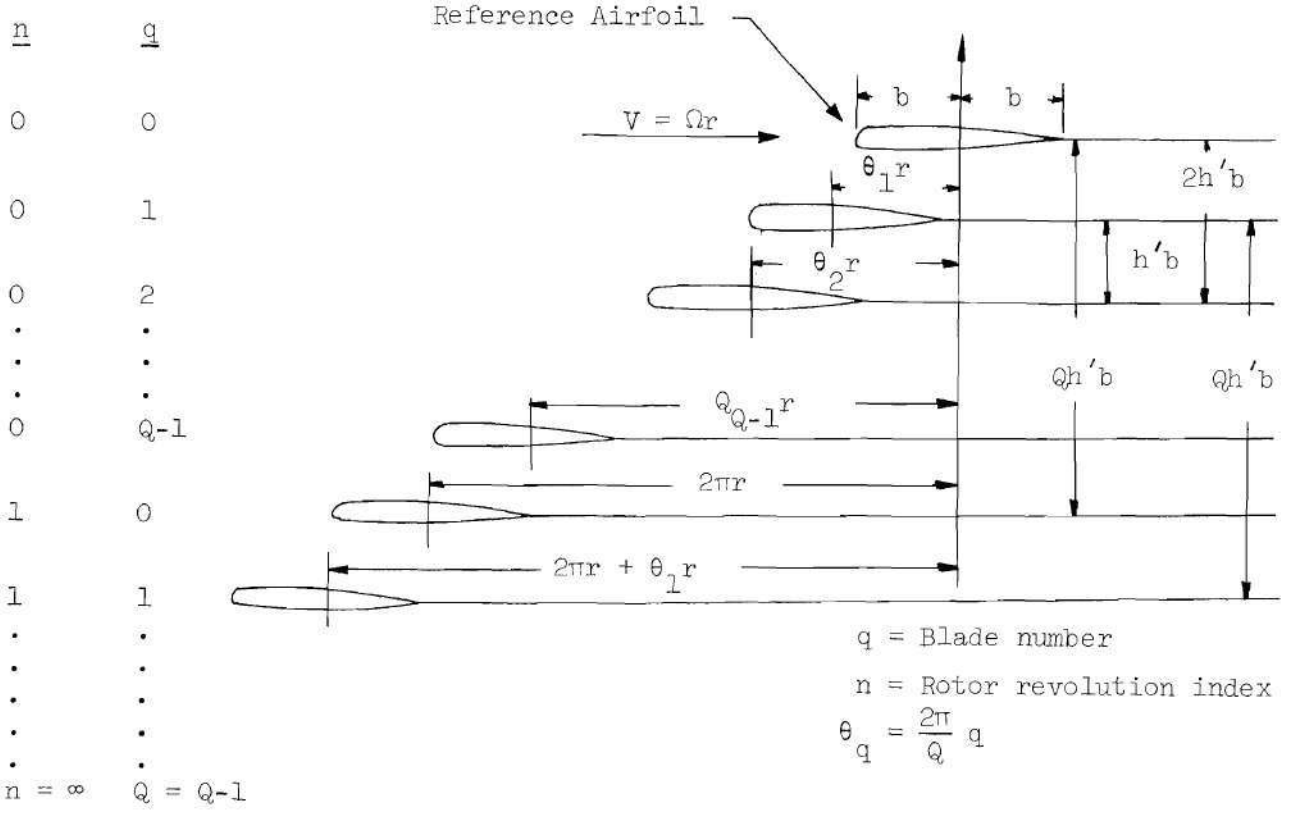

Figure 5. Compressible Aerodynamic Model for a Multibladed Rotor

associated with a pressure discontinuity. This necessitated the use of artificial airfoils to generate the layers of wake below the reference airfoil. As a result, the lower wakes include the effects of compressibility due to their finite distance from the reference airfoil. Hammond was able to reduce his model to that used by Jones and Rao by allowing the wake airfoils to lead the reference airfoil by an infinite distance. Thus, the time delay between the initiation of a disturbance and the time it is felt at the reference airfoil is thus lost and the wake layers appear as incompressible wakes. This is exactly the result obtained by Jones and Rao. Figure 6 illustrates aerodynamic derivatives computed by Hammond [20] and Jones and Rao [18] at Mach numbers of 0.0, 0.6 and 0.8. It is obvious that different results were obtained for the two flow models. The importance of these differences can only be established on the basis of how they influence flutter speed. Of equal importance is the economical efficiency relative to the accuracy of each theory in flutter speed prediction.

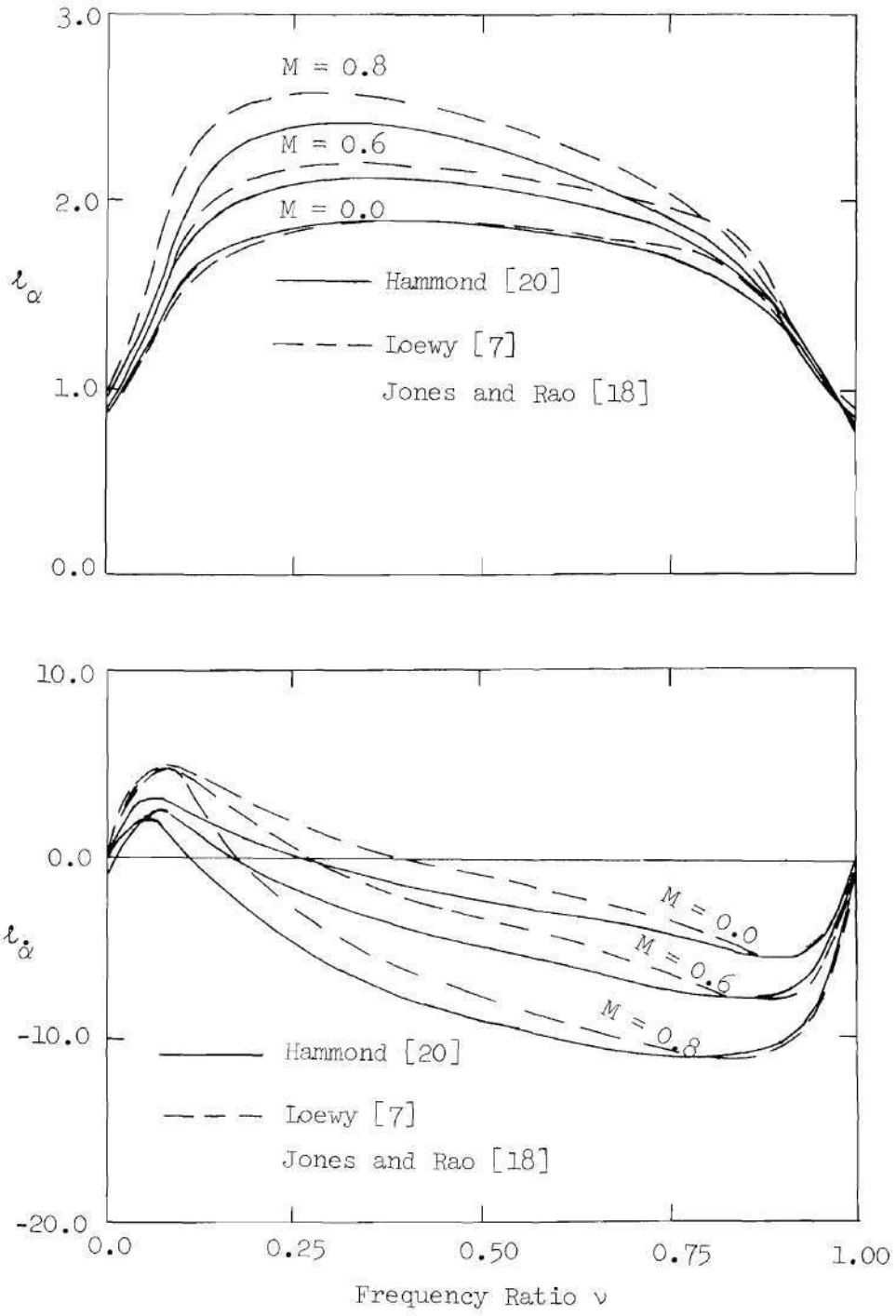

Figure 6. Variation of the Aerodynamic Coefficients ℓ_α and $\ell_{\dot{\alpha}}$ with Frequency Ratio (k = 0.10, h' = 2.0)

CHAPTER III

THEORETICAL DEVELOPMENT

In this chapter, the equations of motion are derived and used to formulate the flutter determinant. The solution of the flutter equations is discussed. The appropriate differences between a helicopter rotor and fixed wing analysis are examined.

Equations of Motion

The displacement of a typical section of the rotor at a radial station y is shown in Figure 7. This two-dimensional section is subject to inertial, elastic and aerodynamic loads. An element of mass per unit area, $\bar{m}$, is subject to a centrifugal force

$$dF_c = \bar{m}\,\Omega^2\, y\, dx$$

Following the suggestion of Rosenberg [2], the normal component of centrifugal force is

$$\left(dF_c\right)_n = \bar{m}\,\Omega^2\, y \sin\theta\, dx$$

which for small elastic displacements, is approximated by

$$\left(dF_c\right)_n = \bar{m}\,\Omega^2\, y\, \theta\, dx$$

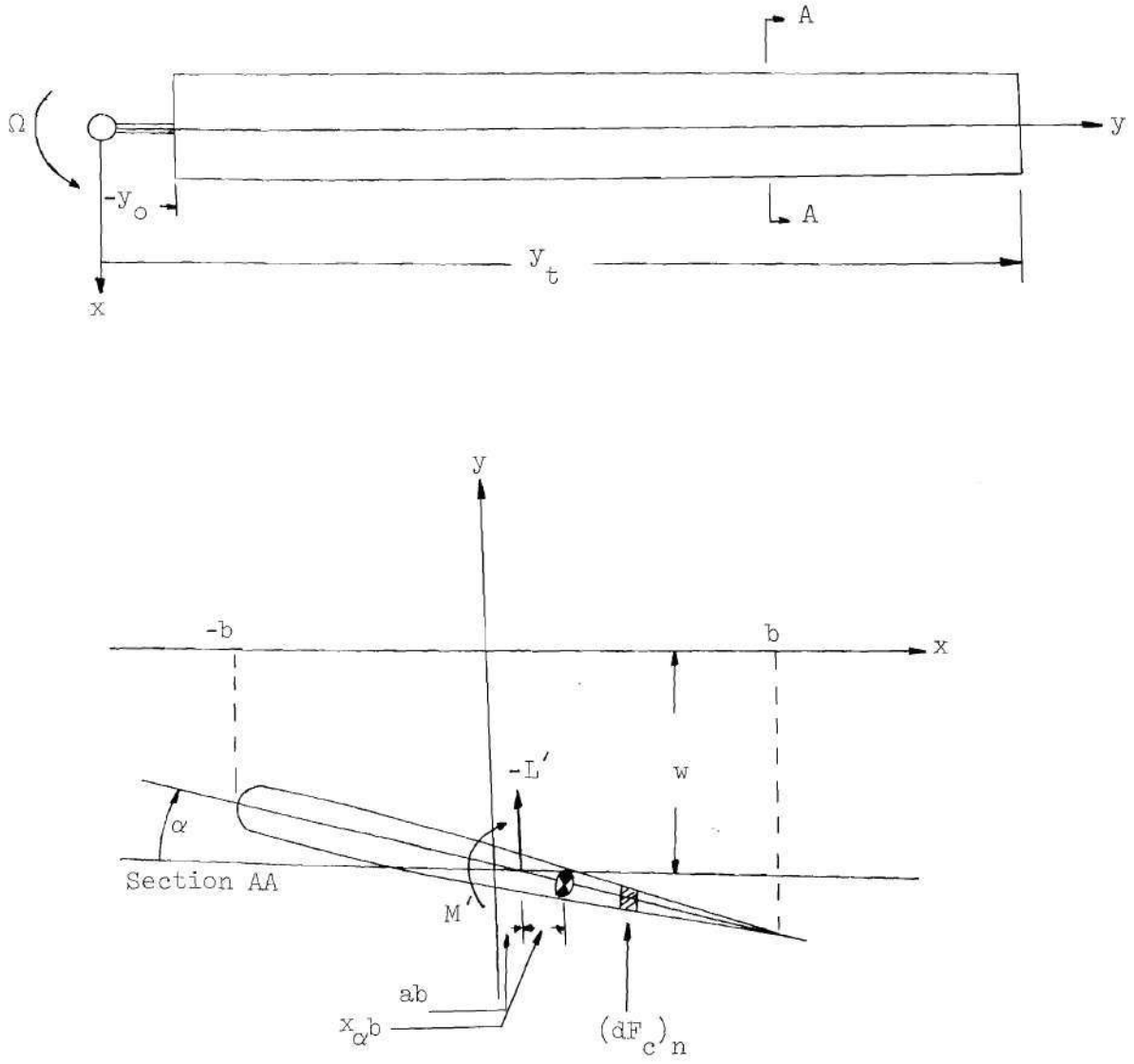

Figure 7. Notation for Blade Displacement

This component of centrifugal force is shown in Figure 8. The total translatory displacement of an element of mass $\bar{m}$ is $\left[w + (x - ab)\alpha\right]$ and θ is approximately given by

$$\theta = \left[w + (x - ab)\alpha\right]/y$$

The above expression for θ is identically true only for blades whose translatory deflection is caused entirely by a flapping deflection about a hinge located at the root. For blades which deflect elastically and which are hingless this expression is an approximation as shown in Figure 8. Using the above expression the normal component of centrifugal force is approximated by

$$\left(dF_c\right)_n = \bar{m}\,\Omega^2 \left[w + (x - ab)\alpha\right]dx$$

and the centrifugal moment about the elastic axis is

$$dM_c = \bar{m}\,\Omega^2\,(x - ab)\left[w + (x - ab)\alpha\right]dx$$

A chordwise integration gives the centrifugal force and moment per unit span about the elastic axis at a spanwise station y.

$$F_c' = m\,\Omega^2\,w + S_\alpha\,\Omega^2\,\alpha \qquad (1)$$

$$M_c' = S_\alpha\,\Omega^2\,w + I_\alpha\,\Omega^2\alpha$$

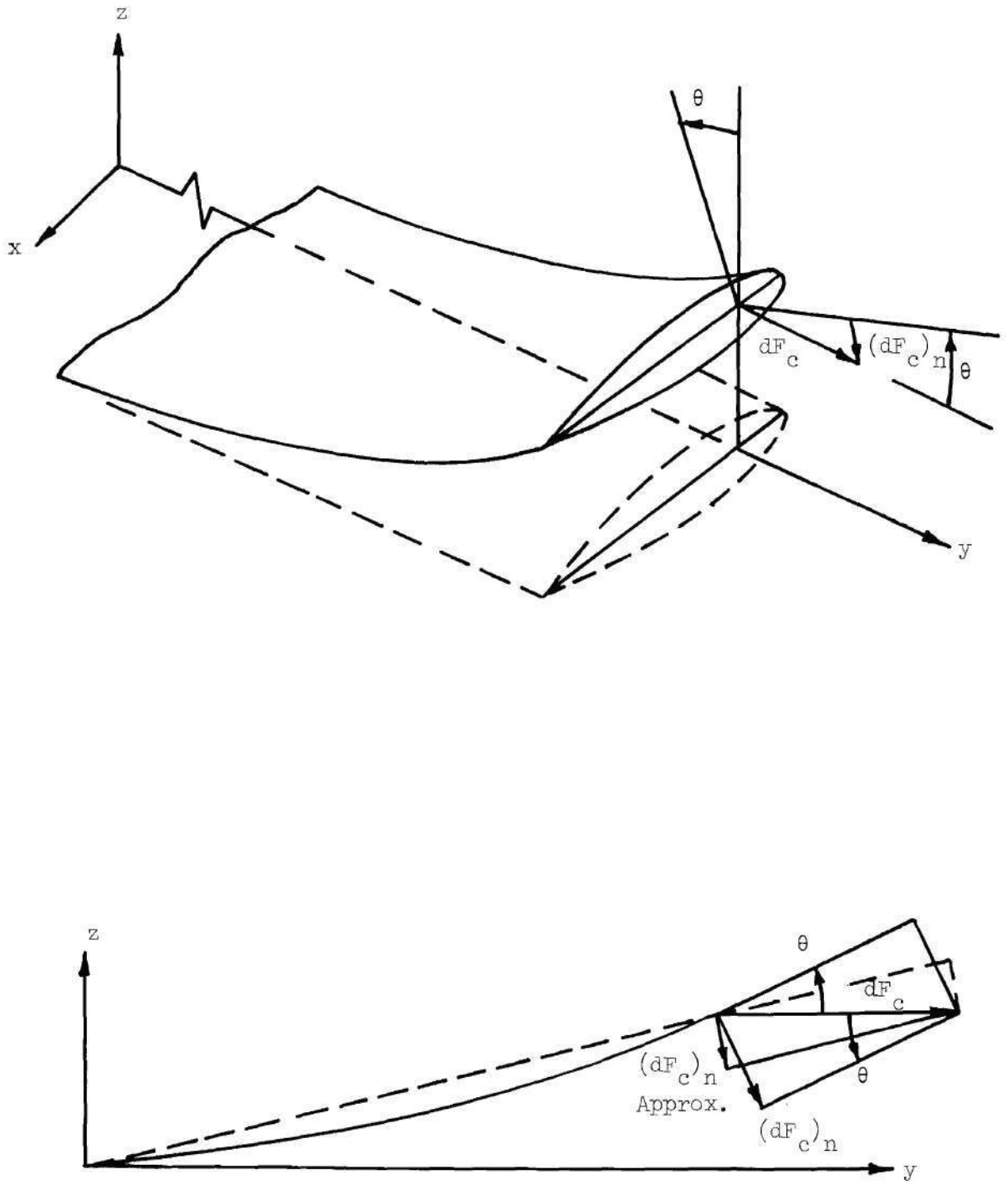

Figure 8. Approximation of the Vertical Component of Centrifugal Force

where

$$m = \int_{-b}^{b} \bar{m}\, dx \tag{2}$$

$$S_\alpha = \int_{-b}^{b} (x - ab)\, \bar{m}\, dx$$

$$I_\alpha = \int_{-b}^{b} (x - ab)^2\, \bar{m}\, dx$$

Equations (1) are considered as centrifugal body forces per unit span which approximate the inertial loads due to blade rotation.

At a radial station y the kinetic energy per unit span for a non-rotating beam is

$$T' = \frac{1}{2} \int_{-b}^{b} \left(\frac{\partial z}{\partial t}\right)^2 \bar{m}\, dx \tag{3}$$

where

$$z = -\left[w + (x - ab)\alpha\right] \tag{4}$$

substituting Equation (4) into Equation (3) and using the definitions of Equation (2) gives

$$T' = \frac{1}{2}\left[m\,\dot{w}^2 + 2\,S_\alpha\dot{\alpha}\dot{w} + I_\alpha\dot{\alpha}^2\right] \tag{5}$$

The total kinetic energy is obtained by integrating over the span

$$T = \frac{1}{2}\int_{y_o}^{y_t}\left[m\,\dot{w}^2 + 2\,S_\alpha\dot{\alpha}\dot{w} + I_\alpha\dot{\alpha}^2\right]dy \tag{6}$$

The potential energy of the internal forces may be written as the total of the strain energy in bending and torsion as

$$U = \frac{1}{2}\int_{y_o}^{y_t} EI(y)\left[\frac{\partial^2 w}{\partial y^2}\right]^2 dy \tag{7}$$

$$+ \frac{1}{2}\int_{y_o}^{y_t} GJ(y)\left[\frac{\partial\alpha}{\partial y}\right]^2 dy$$

A matrix integration formulation of the coupled bending-torsional natural vibration of a rotating blade is presented in Appendix A. Unfortunately available computer facilities precluded the use of this method in the present study. The alternative procedure used in this study was to conduct a conventional lumped parameter vibration analysis for the coupled bending-torsion modes of a non-rotating blade. If the coupled bending-torsional modes of the

non-rotating blade are used as assumed modes for the rotating blade the displacement at a radial station may be approximated as a superposition of the contributions of the various modes.

$$h(y,t) = \sum_{i=1}^{M} h_i(y)\ \xi_i(t) \tag{8}$$

$$\alpha(y,t) = \sum_{i=1}^{M} \alpha_i(y)\ \xi_i(t)$$

Equations (8) may be written in matrix form as

$$\left\{\frac{h}{\alpha}\right\} = \left[\phi\right] \left\{\xi\right\} \tag{9}$$

where $\left[\phi\right]$ is the eigenvector matrix for the normal modes of the non-rotating beam. Substituting Equations (8) into Equation (6) and using the orthogonality of the normal modes the kinetic energy may be expressed in non-dimensional form as

$$T = \frac{1}{2}\pi\rho\, b_t^4\, R \sum_{i=1}^{M} G_i\, \dot{\xi}_i^2 \tag{10}$$

with

$$G_i = \int_{\eta_o}^{\eta_t} \left(\mu h_i^2 + \mu r_\alpha^2 \alpha_i^2 + 2 \mu x_\alpha h_i \alpha_i \right) d\eta \tag{11}$$

where the following nondimensional parameters have been introduced

$$h = w/b_t \tag{12}$$

$$\mu = m/\pi \rho b_t^2$$

$$x_\alpha = S_\alpha/mb_t$$

$$r_\alpha^2 = I_\alpha/mb_t^2$$

$$\eta = y/R$$

Using the normal modes the potential energy is expressible as a function of the generalized coordinates (Reference [4]).

$$U = \frac{1}{2} \pi \rho b_t^4 R \sum_{i=1}^{M} G_i \omega_i^2 \xi_i^2 \tag{13}$$

Lagrange's equations of motion may be written as

$$\frac{d}{dt}\left(\frac{\partial T}{\partial \dot{\xi}_i}\right) + \frac{\partial U}{\partial \xi_i} = Q_i \qquad (14)$$

The generalized forces Q_i can be determined from the virtual work done by the aerodynamic loads and the centrifugal body forces. Thus if L' is the lift per unit span, M' is the torsional moment about the elastic axis per unit span, the virtual work done during a virtual displacement of the i^{th} mode is

$$\delta W_i = R\,\delta\xi_i \int_{\eta_o}^{\eta_t} \left(L' b_t h_i + M'\alpha_i - F_c' b_t h_i - M_c' \alpha_i\right) d\eta \qquad (15)$$

and the generalized force is determined as

$$Q_i = \frac{\delta W_i}{\delta \xi_i}$$

Using the following expressions given by Smilg and Wasserman [21] for a two-dimensional airfoil experiencing simple harmonic motion

$$L' = \pi\rho b^3\omega^2 \left\{ L_h \frac{w}{b} + \left[L_\alpha - L_h \left(\frac{1}{2} + a \right) \right] \alpha \right\} \tag{16}$$

$$M' = \pi\rho b^4\omega^2 \left\{ \left[M_h - L_h \left(\frac{1}{2} + a \right) \right] \frac{w}{b} \right.$$

$$\left. + \left[M_\alpha - \left(L_\alpha + M_h \right) \left(\frac{1}{2} + a \right) + L_h \left(\frac{1}{2} + a \right)^2 \right] \alpha \right\}$$

the generalized forces can be obtained from Equation (15). The two-dimensional aerodynamics are applied in a "strip theory" fashion. It should also be noted that when the centrifugal force and moment, given by Equation (1), are substituted into the integral of Equation (15) the orthogonal property of the normal modes simplifies the result. The final expression for the generalized forces due to simple harmonic motion can be written as

$$Q_i = \pi\rho b_t^4 R \left(\omega^2 \sum_{j=1}^{M} A_{ij} \xi_j - \Omega^2 G_i \xi_i \right) \tag{17}$$

The terms, G_i, are given by Equation (11), and the aerodynamic terms, A_{ij}, can be expressed as follows

$$A_{ij} = \int_{\eta_o}^{\eta_t} \left\langle \left(\frac{b}{b_t}\right)^2 L_h \, h_i \, h_j \right. \tag{18}$$

$$+ \left(\frac{b}{b_t}\right)^3 \left[L_\alpha - L_h \left(\frac{1}{2} + a\right) \right] h_i \, \alpha_j$$

$$+ \left(\frac{b}{b_t}\right)^3 \left[M_h - L_h \left(\frac{1}{2} + a\right) \right] \alpha_i \, h_j$$

$$\left. + \left(\frac{b}{b_t}\right)^4 \left[M_\alpha - \left(M_h + L_\alpha\right) \left(\frac{1}{2} + a\right) + L_h \left(\frac{1}{2} + a\right)^2 \right] \alpha_i \alpha_j \right\rangle d\eta$$

Substituting Equations (10), (13) and (17) into Equation (14) yields a set of M equations which can be written in matrix form as

$$\left[G\right] \left\{\ddot{\xi}\right\} + \left[\omega_i G\right] \left\{\xi\right\} \tag{19}$$

$$= \omega^2 \left[A\right] \left\{\xi\right\} - \Omega^2 \left[G\right] \left\{\xi\right\}$$

Assuming simple harmonic motion for each of the normal modes, as was presumed for the aerodynamic terms, of the form

$$\xi = \bar{\xi} \, e^{i\omega t}$$

and defining a frequency ratio parameter as

$$\nu = \omega/\Omega$$

Equation (19) becomes

$$\left[G\right]\left\{\bar{\xi}\right\} - \left[\left(\frac{\omega_i}{\omega}\right)^2 G\right]\left\{\bar{\xi}\right\} \tag{20}$$

$$-\frac{1}{\nu^2}\left[G\right]\left\{\bar{\xi}\right\} + \left[A\right]\left\{\bar{\xi}\right\} = \left\{0\right\}$$

The matrix elements in Equation (20) are integrals over the span which can be evaluated numerically. Introducing a discretized blade model provides an approximate method of evaluating these integrals in matrix form. The blade is divided into an even number of equal segments. If the number of segments is $n - 1$, this will define n control points at which the blade properties are known. Applying Simpson's rule, a matrix of weighting numbers can be formulated (Reference [4]) as

$$\left[\bar{W}\right] = \frac{1}{3(n-1)} \begin{bmatrix} 1 & & & & & & \\ & 4 & & & & & \\ & & 2 & & & & \\ & & & 4 & & & \\ & & & & \ddots & & \\ & & & & & 4 & \\ & & & & & & 1 \end{bmatrix}$$

to accomplish the numerical integration. If $\{\phi\}$ is a column of the modal matrix $[\phi]$ of Equation (9) and

$$[\phi] = \{\phi\}^T$$

then the elements of $[G]$ as defined by Equation (11) can be determined as

$$G_i = [\phi][H][W]\{\phi\} \tag{21}$$

where

$$\left[W_{\searrow}\right] = \left[\begin{array}{c|c} \left[\bar{W}_{\searrow}\right] & \left[0\right] \\ \hline \left[0\right] & \left[\bar{W}_{\searrow}\right] \end{array}\right]$$

and

$$\left[H\right] = \left[\begin{array}{cc|cc} \mu_1 & & (\mu x_\alpha)_1 & \\ & \ddots & & \ddots \\ & \mu_n & & (\mu x_\alpha)_n \\ \hline (\mu x_\alpha)_1 & & (\mu r_\alpha^2)_1 & \\ & \ddots & & \ddots \\ & (\mu x_\alpha)_n & & (\mu r_\alpha^2)_n \end{array}\right] \tag{22}$$

In a similar fashion the matrix $[A]$, whose elements are defined by Equation (18), can be determined as

$$[A] = [\phi]^T [B_1] [C]^T [E] [C] [B_2] [W] [\phi] \tag{23}$$

where

$$[B_1] = \begin{bmatrix} \left(\frac{b}{b_t}\right)^3_1 & & & \\ & \ddots & & \\ & & \left(\frac{b}{b_t}\right)^3_n & \\ & & & \left(\frac{b}{b_i}\right)^4_1 \\ & & & & \ddots \\ & & & & & \left(\frac{b}{b_t}\right)^4_n \end{bmatrix} \tag{24}$$

$$[C] = \begin{bmatrix} 1 & & & -(\frac{1}{2}+a)_1 \\ & \ddots & & & \ddots \\ & & 1 & & & -(\frac{1}{2}+a)_n \\ & & & 1 & & \\ & & & & \ddots & \\ & & & & & 1 \end{bmatrix} \tag{25}$$

$$[E] = \begin{bmatrix} (L_h)_1 & & & (L_\alpha)_1 \\ & \ddots & & & \ddots \\ & & (L_h)_n & & & (L_\alpha)_n \\ (M_h)_1 & & & (M_\alpha)_1 \\ & \ddots & & & \ddots \\ & & (M_h)_n & & & (M_\alpha)_n \end{bmatrix} \tag{26}$$

$$\left[B_2\right] = \begin{bmatrix} \left(\frac{b_t}{b}\right)_1 & & & \\ & \ddots & & \\ & & \left(\frac{b_t}{b}\right)_n & \\ & & & 1 \end{bmatrix} \qquad (27)$$

Equations (21) to (27) are used with the modal matrix $\left[\phi\right]$ of Equation (9) to determine the matrix elements of Equation (20). It may be noted that in Equation (20) the generalized centrifugal force matrix is proportional to the generalized mass matrix. This implies that the net effect of incorporating the centrifugal force by Rosenberg's [2] approximation is to simply reduce the effective generalized mass of all the normal modes.

In order to facilitate the solution of these flutter equations, artificial structural damping is introduced. A structural damping constant, g , may be included by the approximation of replacing ω_i^2 by $\omega_i^2(1 + ig)$ in Equation (20).

$$\left(\left[1 - \left(\frac{\omega_i}{\omega}\right)^2 \left(1 + ig\right) \right] \left[G\right] + \left[A\right] - \frac{1}{\nu^2} \left[G\right] \right) \left\{\bar{\xi}\right\} = \left\{0\right\} \qquad (28)$$

The necessary and sufficient condition for a non-trival solution of Equation (28) is that the determinant of the coefficient matrix vanish.

The representation of the inertial loads due to blade rotation and the use of a discretized model are the essential approximations in the development of Equation (28). Therefore, the solutions provide only an approximation of the aeroelastic instability of a helicopter rotor.

The major concern of this research is the examination of recent aerodynamic theories applicable to rotor flutter prediction in subsonic flow. The generalized aerodynamic loads are present in Equation (28) as the matrix $[A]$. Equation (23) illustrates that the above approximations influence the aerodynamic loads only through the modal matrix $[\phi]$. However, $[\phi]$ is relatively insensitive to rotor speed [22]. Therefore, for the purpose of a qualitative comparison of aerodynamic representations, Equation (28) is adequate.

An alternate formulation of the coupled bending-torsion free vibration of a rotor blade is presented in Appendix A. This formulation is based on a recent study by Hunter [23] of the natural bending vibrations characteristic of propeller blades. Excellent results were obtained using this method for the natural frequencies and mode shapes of a rotor blade. Unfortunately, available computer facilities precluded the use of this method in the present study. The limited numerical results obtained in this investigation and the comprehensive results of Hunter [23] for propeller blades indicate that this method

could be used successfully for design and parametric studies of helicopter rotors.

Flutter Determinant

The necessary and sufficient condition for a non-trivial solution of Equation (28) is that the determinant of the coefficient matrix vanish. Applying this condition to Equation (28) yields

$$|F(\lambda)| = \begin{vmatrix} F_{11} - \lambda & F_{12} & \cdots & F_{1M} \\ F_{21} & F_{22} - \lambda & \cdots & F_{2M} \\ \cdot & \cdot & & \cdot \\ \cdot & \cdot & & \cdot \\ \cdot & \cdot & & \cdot \\ F_{M1} & F_{M2} & & F_{MM} - \lambda \end{vmatrix} = 0 \qquad (29)$$

where

$$F_{ij} = \begin{cases} \left(\frac{A_{ij}}{G_i} - \nu^{-2} + 1\right)\left(\frac{\omega_1}{\omega_i}\right)^2 & i = j \\ \frac{A_{ij}}{G_i}\left(\frac{\omega_1}{\omega_i}\right)^2 & i \neq j \end{cases} \qquad (30)$$

and

$$\lambda = \left(\frac{\omega_1}{\omega}\right)^2 \left(1 + ig\right) \tag{31}$$

Following the suggestion of Smilg and Wasserman [21], the determinant may be expanded to form a polynomial in λ. The flutter determinant, Equation (29), and its corresponding polynomial is of order M where M is the number of modes. In general the coefficients and roots are complex numbers. If M is large, the expansion of Equation (29) by cofactors is inefficient. In this analysis, the coefficients of the characteristic polynomial were obtained by the Leverrier-Faddeev method [24]. Numerous methods of obtaining the roots of the characteristic polynomial are available [24].

Solution of the Flutter Equations

By specifying the spanwise variation in the rotor blade geometric, inertial, and elastic properties, G_i in Equation (30) is determined from Equation (21). The elements A_{ij} of the aerodynamic matrix, Equation (23), may be evaluated if the spanwise variation of the aerodynamic coefficients L_h, L_α, M_h, and M_α are known. These aerodynamic coefficients are complicated functions of Mach number, reduced frequency, inflow ratio, and frequency ratio which may be expressed as functions of the spanwise variable η.

The aerodynamic coefficients are determined from the compressible unsteady aerodynamic theories of Hammond [20], and Jones and Rao [18]

in a strip theory fashion. The influence of the two different mathematical models on flutter calculations is established. In addition, the relative accuracy and economical efficiency of each theory are considered.

In order to reduce the computation of aerodynamic coefficients to a tractable form, tables of the coefficients were constructed. A series of tables were computed for a representative number of tip Mach numbers. For a specified blade, the tip Mach number yields the local value at chosen spanwise stations. In this analysis, eight stations were used in constructing the tables. Aerodynamic coefficients at additional stations were obtained by interpolation. Spanwise interpolation of the coefficients was quite satisfactory. However, extreme care is required for interpolation on reduced frequency. Reduced frequency and frequency ratio are related through the blade geometry as

$$\nu = k_t \frac{R}{b_t} \tag{32}$$

Thus, interpolation of reduced frequency involves a variation in frequency ratio. As discussed earlier, the aerodynamic coefficients vary radically with frequency ratio near interger multiples of the number of blades. Satisfactory results were obtained by specifying a spectrum of tip reduced frequencies incremented at 0.0035 with $R/b_T = 23.0$.

The local inflow velocity was allowed to vary spanwise and

was approximated by a combined axial momentum and blade element theory [25]

$$h' = \frac{2\pi R}{Qb}\left[\frac{U}{2} + \frac{\bar{a}\sigma}{16}\cos\alpha_t - \sqrt{\left(\frac{U}{2} + \frac{\bar{a}\sigma}{16}\cos\alpha_t\right)^2 + \frac{\bar{a}\sigma\eta}{8}\sin\alpha_t}\right] \qquad (33)$$

The flutter speed for a helicopter rotor may be determined, as in the fixed wing case, by iteration of the characteristic polynomial. The solutions are expressed in terms of the damping parameter, g , and oscillatory frequency, ω , of Equation (31).

The flutter speed is determined by specifying a tip Mach number and varying tip reduced frequency. This in turn specifies frequency ratio, local Mach number and local reduced frequency where Equation (33) is used to approximate the local inflow ratio. For each tip reduced frequency, Equation (31) determines the damping parameter and oscillatory frequency of each mode. A non-dimensional velocity is defined as

$$\frac{V_t}{b_t\omega_1} = \frac{1}{k_t}\left(\frac{\omega}{\omega_1}\right) \qquad (34)$$

and plotted versus the damping parameter for each mode. The flutter speed is determined when the damping constant of one of the modes is zero. This process is repeated for various tip Mach numbers.

The non-dimensional flutter speed as defined in Equation (34) is a conventional fixed wing parameter which has been adopted for use in most helicopter flutter analyses. It can be interpreted as a non-dimensional rotor speed.

In this analysis, compressible aerodynamics are used with an iteration procedure based on advanced selection of Mach number and reduced frequency. Thus, the additional parameter, atmospheric density is introduced by a selection of μ . The results of this iteration procedure correspond to a particular altitude. Thus, only one altitude is associated with each flutter speed. Mach number and flutter speed can be plotted for various values of μ and points of intersection with a particular altitude line establishes the flutter boundary.

CHAPTER IV

DISCUSSION OF RESULTS

In the previous chapters the importance of compressible unsteady aerodynamic theory has been discussed. In this chapter the compressible theories of Hammond [20], and Jones and Rao [18] are utilized to predict helicopter rotor flutter speeds. The influence of the two different mathematical models on flutter calculations is established. Numerical results of predicted flutter speed are compared with available experimental results.

Comparison of Theory with Experiment

An extensive review of the literature yielded only limited experimental flutter data to corroborate the predicted flutter speeds. Brooks and Baker [26] conducted an experimental investigation of the effects of tip Mach number on the flutter of helicopter rotor blade models. The blades used in the test were designed to be geometrically representative of normal helicopter configurations, and to flutter at speeds which would yield data at Mach numbers where compressibility effects might become important over a range of pitch angles. Correlation could be attempted with only part of the results, since a large portion of their data was obtained with high pitch settings, so that the blade was undergoing stall flutter. Correlation is made with the blade model designated as blade 2 (R) in Reference [26]. This model had an NACA 23012 airfoil section with uniform spanwise blade properties

which are tabulated in Reference [26]. Table 1 presents the comparison of experimental and calculated flutter speeds. The non-dimensional flutter speed includes the ratio $\sqrt{\rho/\rho_o}$ which was introduced to reduce scatter of the experimental results obtained at different densities of the testing medium. The calculated flutter speeds in Table 1 were obtained using five modes. These modes included first torsion and first, second, third, and fourth bending. The first torsional frequency occurred between the second and third bending frequency. Examination of the calculated flutter data indicated that five modes were sufficient for this blade. Flutter was observed to occur as a coalescence of the first torsional mode with the second bending mode. The higher modes were strongly damped.

The results in Table 1 indicate that the aerodynamic theories of Hammond [20], and Jones and Rao [18] yield essentially the same flutter speed. The predicted speed is in good agreement with the experimental values. The predicted flutter speed without the wake in general yields less agreement. The data in Table 1 is based on a blade pitch angle of 7.2°. Lower pitch angles would produce larger errors when the wake is neglected.

Typical damping plots used to obtain the data of Table 1 are shown in Figures 9 and 10. The oscillatory behavior of the damping parameter is to be expected from the discussion of the aerodynamic models. The abscissa of these plots corresponds to the non-dimensional tip speed which is a measure of rotor rotational speed. Therefore, as the rotational speed is increased, the aerodynamic damping of the

Table 1. Comparison of Experimental and Calculated Flutter Speeds

		Brooks and Baker [26]	Hammond [20]	Jones and Rao [18]	Neglecting Wake [18]
M_t	$\sqrt{\rho/\rho_o}$	$\frac{V_t}{b\omega_\alpha}\sqrt{\rho/\rho_o}$	$\frac{V_t}{b\omega_\alpha}\sqrt{\rho/\rho_o}$	$\frac{V_t}{b\omega_\alpha}\sqrt{\rho/\rho_o}$	$\frac{V_t}{b\omega_\alpha}\sqrt{\rho/\rho_o}$
.416	1.000	6.3	6.12	6.06	6.6
.433	.985	6.5	6.04	6.04	6.6
.443	.948	6.01	5.98	5.98	6.5
.667	.966	5.58	5.89	5.86	6.37
.693	1.028	5.53	5.92	5.9	6.48

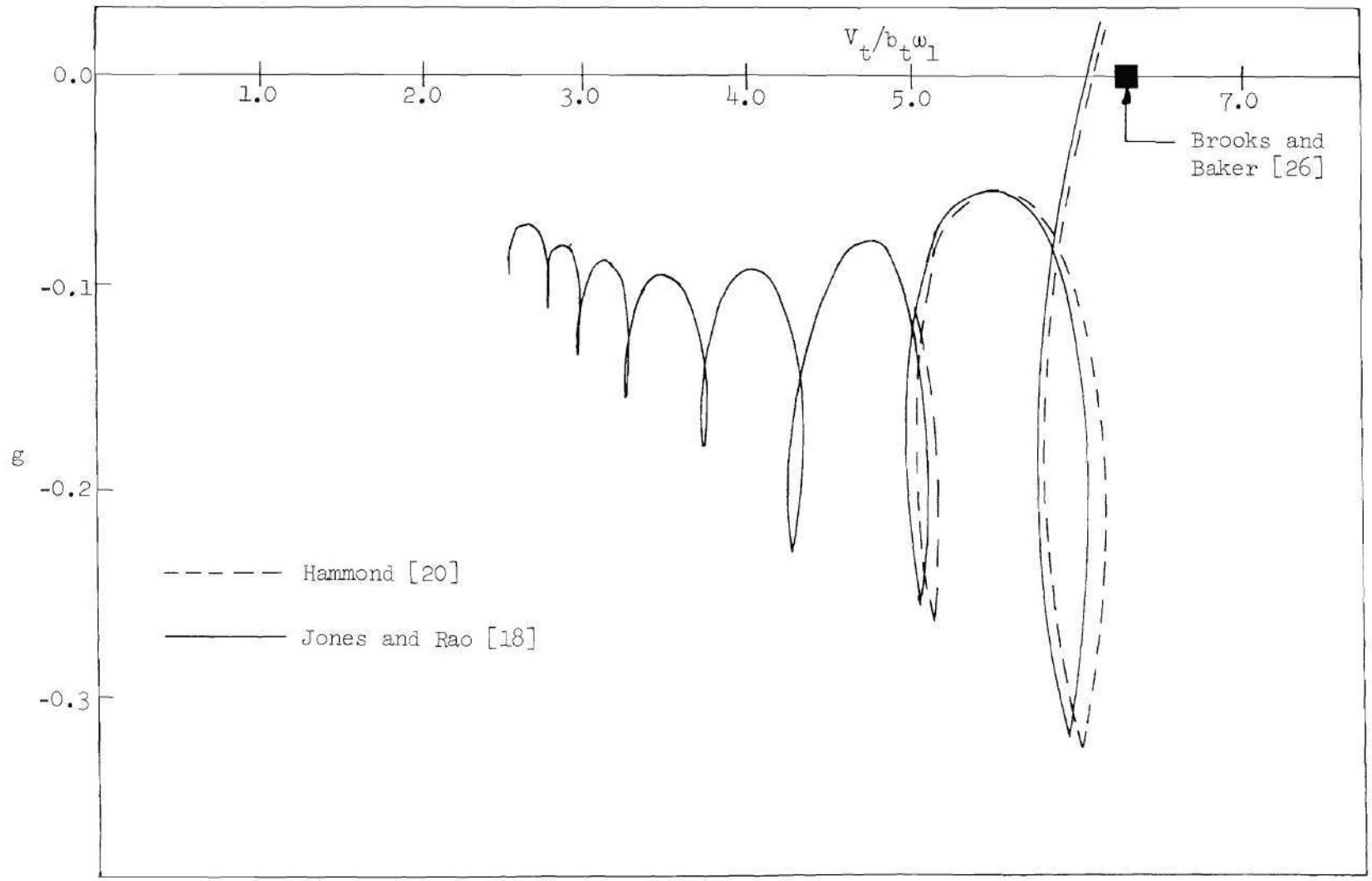

Figure 9. Structural Damping Constant for a Model Helicopter Rotor at M = 0.416 as a Function of Non-dimensional Tip Speed

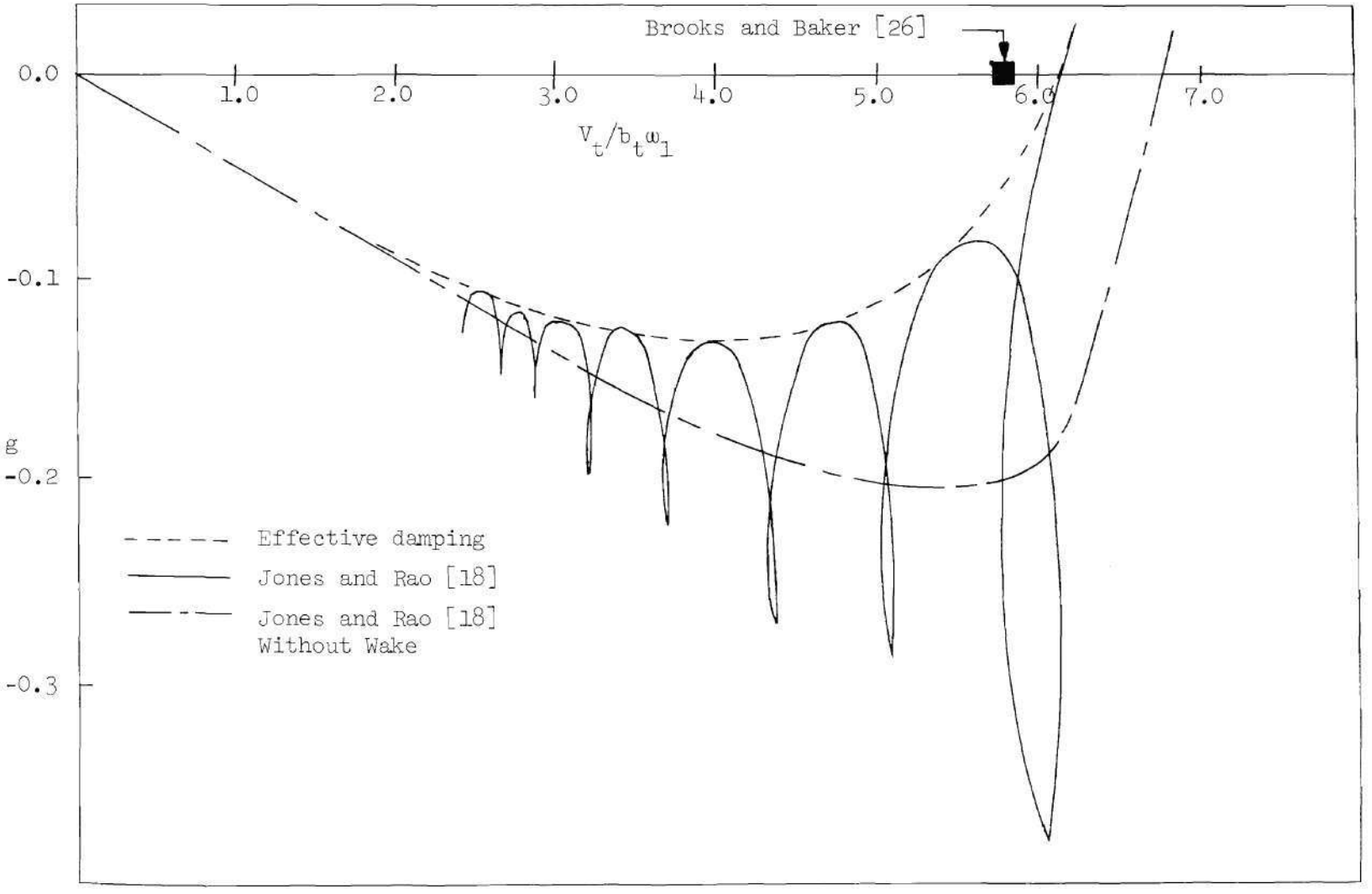

Figure 10. Structural Damping Constant for a Model Helicopter Rotor at M = 0.667 as a Function of Non-dimensional Tip Speed

aeroelastic system oscillates in magnitude until finally a dynamic instability occurs. Associated with each point on the damping plot, there is a corresponding frequency ratio. Although it is not indicated in the figures, the oscillation of the damping constant continues after the instability is experienced. It is suggested that the flutter speed for a helicopter rotor at low inflow be based on the curve labeled effective damping in Figure 10 where it intersects the abscissa. This eliminates the uncertainty associated with the oscillatory damping characteristics.

In order to generate the effective damping curve of Figure 10, it is necessary to establish the oscillatory nature of the actual damping curve. It is necessary to insure that peaks in the damping curve are well defined. Satisfactory definition of the peaks was obtained by varying reduced frequency in increments of 0.0035 or less. The left portion of each peak is well defined but the right portion exhibited abrupt changes in damping with constant increments in reduced frequency. The portions of the oscillatory damping curve away from the peaks are of little significance with respect to flutter speed determination.

Evaluation of Computational Efficiency

The aerodynamic theory of Jones and Rao [18] requires significantly less computer time than the theory of Hammond [20]. The computer time required to compute the aerodynamic coefficients in Equation (16) using Hammond's theory was found to be a strong function of Mach number.

In contrast, the computer time required by the theory of Jones and Rao was virtually independent of Mach number. Numerical calculations using Hammond's theory on a Univac 1108 at Mach numbers of 0.0 and 0.80 required 170.0 and 440.0 seconds respectively. The corresponding computer times using the theory of Jones and Rao was 5.0 and 6.0 seconds respectively. This significant difference in computer time can be attributed to differences in numerical methods and the mathematical models of the rotor wake.

CHAPTER V

CONCLUSIONS AND RECOMMENDATIONS

The compressible unsteady aerodynamic theories of Hammond [20] and Jones and Rao [18] were utilized in conjunction with a flutter analysis to establish a flutter criteria for helicopter rotors. The influence of the two different mathematical models on flutter calculations was established.

Conclusions

1. The compressible unsteady aerodynamic theories of Hammond [20] and Jones and Rao [18] yield essentially the same results for flutter speed.

2. The aerodynamic theory of Jones and Rao [18] requires a significantly less amount of computer time than the theory of Hammond [20].

3. An analysis of the aeroelastic instability of a helicopter rotor at low inflow should include wake effects.

4. The flutter speed for a helicopter rotor should be determined from the curve labeled effective damping in Figure 10.

Recommendations

A number of general suggestions are offered concerning the directions future studies of the rotary wing flutter problem might take.

1. Probably one of the greatest needs is additional experimental flutter data. An experimental program should definitely include the possibility of operating the rotor under compressible flow conditions, since the trend in present helicopter design is toward the high subsonic speed range.

2. An improved vibration analysis should be incorporated in the flutter analysis. This would facilitate the study of a wide variety of rotor configurations. The vibration analysis developed in Appendix A could be modified to incorporate the inplane degree of freedom, spanwise variation in blade twist and a variety of root boundary conditions.

3. An experimental program should be conducted to validate the normal mode method of vibration analysis for helicopter rotors. Such a program could be conducted by varying rotor speed in a vacuum chamber.

4. An obvious extension of the present study is an unsteady compressible three-dimensional aerodynamic theory applicable for flutter analyses at forward speeds. This type of theory is desirable in order to more realistically represent the aeroelastic characteristics of helicopter rotors.

APPENDIX A

INTEGRATING-MATRIX METHOD FOR DETERMINING THE COUPLED BENDING-TORSIONAL NATURAL VIBRATION CHARACTERISTICS OF HELICOPTER ROTOR BLADES

In this appendix, a coupled bending-torsional natural vibration analysis is presented. This formulation is similar to a recent study by Hunter [23] of the natural bending vibration characteristics of propeller blades. In Hunter's method, an integrating matrix is developed as the basis for the method of solution. The integrating matrix is a means of numerically integrating a function that is expressed in terms of the values of the function at equal increments of the independent variable. It is derived by expressing the integrand as a polynomial in the form of Newton's forward-difference interpolation formula.

The solution to the governing differential equations of motion is developed entirely in matrix notation which allows the numerical solution to be developed in a compact and orderly fashion. The matrix differential equations are then integrated repeatedly by using the integrating matrix as an operator. Next, the constants of integration are evaluated by applying the boundary conditions. Finally, the resulting matrix equation is expressed in the familiar concise form of the eigenvalue problem.

Development of the Integrating Matrix

The integrating matrix is a numerical method based on the assumption that the function f(y) may be represented by a polynomial of degree r as

$$f(y) = a_0 + a_1 y + a_2 y^2 + \ldots a_r y^r \qquad \text{(A-1)}$$

Let f_i denote the value of $f(y)$ at the station $y = y_i$ where $i = 0, 1, 2, \ldots, r$. If the stations are assumed to be equally spaced, then $y_i = y_0 + iP$ where P is the spacing interval.

In proceeding with the development of the integrating matrix, it is convenient to choose a specific polynomial as an example. If the function is assumed to be approximated by a third-degree ($r = 3$) polynomial, then Newton's forward-difference interpolation formula of order three can be used as

$$f(y) = g(s)$$

$$= f_0 + \frac{1}{1!} s \Delta^1 f_0 + \frac{1}{2!} s(s-1) \Delta^2 f_0$$

$$+ \frac{1}{3!} s(s-1)(s-2) \Delta^3 f_0$$

where

$$s = (y - y_0)/P$$

$$\Delta^1 f_0 = f(y_0 + P) - f(y_0) = f_1 - f_0$$

$$\Delta^n f_0 = \Delta^{n-1} f(y_0 + P) - \Delta^{n-1} f(y_0)$$

This leads to

$$g(s) = f_0 + s\left(f_1 - f_0\right)$$

$$+ \frac{1}{2}\left(s^2 - s\right)\left(f_2 - 2f_1 + f_0\right)$$

$$+ \frac{1}{6}\left(s^3 - 3s^2 + 2s\right)\left(f_3 - 3f_2 + 3f_1 - f_0\right)$$

Integration of this function with respect to s yields the desired approximate integral of $f(x)$ as

$$\int_{y_i}^{y_j} f(y)dy = P \int_{i}^{j} g(s)ds$$

and for the case of the three intervals between y_0 and y_3 the results is

$$\int_{y_0}^{y_1} f(y)dy = \frac{P}{24}\left(9f_0 + 19f_1 - 5f_2 + f_3\right) \qquad \text{(A-2a)}$$

$$\int_{y_1}^{y_2} f(y)dy = \frac{P}{24}\left(-f_0 + 13f_1 + 13f_2 - f_3\right) \qquad \text{(A-2b)}$$

$$\int_{y_2}^{y_3} f(y)dy = \frac{P}{24}\left(f_0 - 5f_1 + 19f_2 + 9f_3\right) \qquad \text{(A-2c)}$$

The function $f(y)$ may be integrated over a large number of equal length intervals by repeated use of Equation (A-2b). Thus, from Equations (A-2) the numerical integration of $f(y)$ over each of n intervals from y_0 to y_n is given by

$$\left.\begin{aligned}
&\int_{y_0}^{y_1} f(y)dy = \frac{P}{24}\left(9f_0 + 19f_1 - 5f_2 + f_0\right)\\
&\int_{y_1}^{y_2} f(y)dy = \frac{P}{24}\left(-f_0 + 13f_1 + 13f_2 - f_3\right)\\
&\int_{y_2}^{y_3} f(y)dy = \frac{P}{24}\left(-f_1 + 13f_2 + 13f_3 - f_4\right)\\
&\qquad\qquad\vdots\\
&\int_{y_{n-2}}^{y_{n-1}} f(y)dy = \frac{P}{24}\left(-f_{n-3} + 13f_{n-2} + 13f_{n-1} - f_n\right)\\
&\int_{y_{n-1}}^{y_n} f(y)dy = \frac{P}{24}\left(f_{n-3} - 5f_{n-2} + 19f_{n-1} + 9f_n\right)
\end{aligned}\right\} \quad \text{(A-3)}$$

Equation (A-3) may be expressed in matrix notation as

$$\left\{ \int_{y_{i-1}}^{y_i} f(y)dy \right\} = \left[A_3 \right] \left\{ f \right\} \qquad \text{(A-4a)}$$

where

$$\left\{ \int_{y_{i-1}}^{y_i} f(y)dy \right\} = \left\{ \begin{array}{l} 0 \\ \int_{y_0}^{y_1} f(y)dy \\ \int_{y_1}^{y_2} f(y)dy \\ \vdots \\ \int_{y_{n-1}}^{y_n} f(y)dy \end{array} \right\} \qquad \text{(A-4b)}$$

$$\{f\} = \begin{Bmatrix} f_0 \\ f_1 \\ f_2 \\ | \\ | \\ | \\ | \\ | \\ f_n \end{Bmatrix} \qquad \text{(A-5)}$$

$$\left[A_3\right] = \frac{P}{24} \begin{bmatrix} 0 & 0 & 0 & 0 & 0 & 0 & 0 & \cdots & 0 \\ 9 & 19 & -5 & 1 & 0 & 0 & & & | \\ -1 & 13 & 13 & -1 & 0 & 0 & & & | \\ 0 & -1 & 13 & 13 & -1 & 0 & & & | \\ 0 & 0 & -1 & 13 & 13 & -1 & & & | \\ | & & & & & & & & | \\ | & & & & & & & & | \\ | & & & & & & & & | \\ | & & & & & & & & | \\ | & & & & & & & & 0 \\ | & & & & & & 0 & -1 & 13 & 13 & -1 \\ 0 & \cdots & & & & & 0 & 1 & -5 & 19 & 9 \end{bmatrix} \qquad \text{(A-6)}$$

As noted earlier, the matrix $\left[A_3\right]$ is based on a third degree polynomial. In a similar manner, matrices such as this were determined by Hunter based upon polynomials up to seventh degree.

The integral of $f(y)$ from y_0 to y_i may be obtained by merely summing the integrals given for each interval from y_0 to y_i. Thus,

$$\int_{y_0}^{y_i} f(y)dy = \int_{y_0}^{y_1} f(y)dy + \int_{y_1}^{y_2} f(y)dy + \ldots \qquad \text{(A-7)}$$

$$\ldots\ldots + \int_{y_{i-1}}^{y_1} f(y)dy$$

Equation (A-7) is given in matrix notation for $i = 0, 1, 2, \ldots, n$ by

$$\left\{\int_{y_0}^{y_i} f(y)dy\right\} = \left[B\right]\left\{\int_{y_{i-1}}^{y_i} f(y)dy\right\} \qquad \text{(A-8a)}$$

where

$$\left\{ \int_{y_0}^{y_i} f(y)dy \right\} = \left\{ \begin{array}{l} 0 \\ \\ \int_{y_0}^{y_1} f(y)dy \\ \\ \int_{y_0}^{y_2} f(y)dy \\ \\ \vdots \\ \\ \int_{y_0}^{y_n} f(y)dy \end{array} \right\} \qquad \text{(A-8b)}$$

and

$$\left[B\right] = \begin{bmatrix} 1 & 0 & 0 & 0 & \cdots & 0 \\ 1 & 1 & 0 & 0 & & \vdots \\ 1 & 1 & 1 & 0 & & \\ 1 & 1 & 1 & 1 & & \\ \vdots & & & & & \\ & & & & 1 & 0 \\ 1 & \cdots & & & 1 & 1 \end{bmatrix}$$

It may be noted that the first column of $\left[B\right]$ is arbitrary and the ones are chosen for uniformity.

Substituting Equation (A-4a) into Equation (A-8a) and replacing the matrix $\left[A_3\right]$ by the general matrix $\left[A_r\right]$ gives

$$\left\{ \int_{y_0}^{y_i} f(y)dy \right\} = \left[B\right]\left[A_r\right]\left\{f\right\} \tag{A-9}$$

The integrating matrix is defined as

$$\left[I\right] = \left[B\right]\left[A_r\right] \tag{A-10}$$

and Equation (A-9) becomes

$$\left\{ \int_{y_0}^{y_i} f(y)dy \right\} = \left[I\right]\left\{f\right\} \tag{A-11}$$

which is the desired matrix expression. Thus, the premultiplication by the integrating matrix of a column matrix defining the function

$f(y)$ yields the numerical integration of $f(y)$ from y_0 to y_i where $i = 0, 1, 2, \ldots, n$.

By using Newton's forward difference interpolation, the integrand may be represented conveniently by polynomials of any degree. The interpolation formula avoids the solving of a set of simultaneous equations since it implicitly contains the polynomial coefficients in terms of the values of the integrand at each station. Also, the integrating matrix as developed by Hunter [23] can be applied to any number of stations as long as $n \geq r$.

Vakhitov [27] earlier developed a numerical method by a different approach. He developed a matrix formulation based on a combined integrating matrix and differentiating matrix. Matrix operators were approximated over two intervals by passing a parabola through three equally spaced points. Although Vakhitov's method represented a different approach, Hunter's method achieves a higher degree of systematization and applicability.

Equations of Motion

The differential equations of motion for combined bending and torsional deformations of nonuniform rotating beams are developed in detail by Houbolt and Brooks [28]. A subcase of the general equations of motion in Reference [28] is used in this analysis. The following simplifications are made to the general set of equations as presented in Reference [28]:

(a) This subcase is the coupled bending and torsional equations, wherein the inplane degree of freedom is deleted.

(b) The blade is assumed to have zero built-in twist.

(c) The tension axis which is defined as the spanwise locus of the centroids of the cross-sectional area effective in carrying tension is assumed to coincide with the elastic axis.

(d) The component of tensile stress in a plane normal to the elastic axis is assumed to produce a negligible torsional resisting moment.

With the additional assumption of simple harmonic motion, the coupled bending-torsional free vibration equations applicable here are

$$\left(EIw''\right)'' - \left(Tw'\right)' - \Omega^2\left(S_\alpha y\alpha\right)' - \omega^2 mw - \omega^2 S_\alpha \alpha = 0 \tag{A-12}$$

$$\left(GJ\alpha'\right)' - \Omega^2 S_\alpha y w' - \Omega^2\left(I_1 - I_2\right)\alpha + \omega^2 S_\alpha w + \omega^2 I_\alpha \alpha = 0 \tag{A-13}$$

where the prime notation indicates the derivative with respect to y. The axial tension T along the span can be obtained from

$$T' + \Omega^2 my = 0 \tag{A-14}$$

Solution of the Equations of Motion

The coupled differential equations are of different order. The solution may be conveniently formulated by integrating each equation separately, applying appropriate boundary conditions, and then combining the resulting matrix equations into a single partitioned-matrix equation.

Equation (A-12) may be expressed in matrix form as

$$\left\{ \left(\left[EI \right] \left\{ w'' \right\} \right)'' \right\} - \left\{ \left(\left[T \right] \left\{ w' \right\} \right)' \right\} \qquad \text{(A-15)}$$

$$- \Omega^2 \left\{ \left(\left[S_\alpha \right] \left[y \right] \left\{ \alpha \right\} \right)' \right\} - \omega^2 \left[m \right] \left\{ w \right\} - \omega^2 \left[S_\alpha \right] \left\{ \alpha \right\} = \left\{ 0 \right\}$$

where

$$\left[EI \right] = \begin{bmatrix} EI_o & & & \\ & EI_1 & & \\ & & \ddots & \\ & & & EI_n \end{bmatrix} \qquad \text{(A-16a)}$$

$$\left[m \right] = \begin{bmatrix} m_o & & & \\ & m_1 & & \\ & & \ddots & \\ & & & m_n \end{bmatrix} \qquad \text{(A-16b)}$$

$$\left[S_{\alpha}\right] = \begin{bmatrix} S_{\alpha_o} & & & \\ & S_{\alpha_1} & & \\ & & \ddots & \\ & & & S_{\alpha_n} \end{bmatrix} \tag{A-16c}$$

$$\left[T\right] = \begin{bmatrix} T_o & & & \\ & T_1 & & \\ & & \ddots & \\ & & & T_n \end{bmatrix} \tag{A-16d}$$

$$\{w\} = \begin{Bmatrix} w_o \\ w_1 \\ \vdots \\ w_n \end{Bmatrix} \qquad \{\alpha\} = \begin{Bmatrix} \alpha_o \\ \alpha_1 \\ \vdots \\ \alpha_n \end{Bmatrix} \tag{A-16e}$$

Equation (A-15) may be integrated numerically by premultiplying by the integrating matrix $\left[I\right]$. Thus, the integration of the equation yields

$$\left\{ \left(\left[EI\right] \left\{w''\right\} \right)' \right\} - \left[T\right] \left\{w'\right\} \qquad \text{(A-17)}$$

$$- \Omega^2 \left[S_\alpha\right] \left[y\right] \left\{\alpha\right\} - \omega^2 \left[I\right] \left[m\right] \left\{w\right\}$$

$$- \omega^2 \left[I\right] \left[S_\alpha\right] \left\{\alpha\right\} + \left\{K_1\right\} = \left\{0\right\}$$

where $\left\{K_1\right\}$ is a constant of integration matrix consisting of a column of equal elements. The constant of integration matrix may be evaluated for a specific set of boundary conditions. In this formulation, the constant of integration matrix is retained after each repeated application of the integrating matrix. For completeness, these constant of integration matrices will be evaluated for a specific set of boundary conditions following the integration of Equations (A-12) and (A-13).

Equation (A-14) may be written in matrix form as

$$\left[T\right] = - \Omega^2 \left[m\right] \left[y\right] \qquad \text{(A-14a)}$$

Also the second term of Equation (A-17) may be expressed as

$$\left[T\right] \left\{w'\right\} = \left\{ \left(\left[T\right] \left\{w\right\} \right)' \right\} - \left[T'\right] \left\{w\right\} \qquad \text{(A-18)}$$

Substituting Equation (A-14a) into Equation (A-18) and then substituting the result into Equation (A-17) gives

$$\left\{ \left(\left[EI\right] \left\{w''\right\} \right)' - \left(\left[T\right] \left\{w\right\} \right)' \right\} - \Omega^2 \left[m\right] \left[y\right] \left\{w\right\} \qquad \text{(A-19)}$$

$$- \Omega^2 \left[S_\alpha\right] \left[y\right] \left\{\alpha\right\} - \omega^2 \left[I\right] \left[m\right] \left\{w\right\}$$

$$- \omega^2 \left[I\right] \left[S_\alpha\right] \left\{\alpha\right\} + \left\{K_1\right\} = \left\{0\right\}$$

Integrating this matrix differential equation by again operating with the integrating matrix gives

$$\left[EI\right] \left\{w''\right\} - \left[T\right] \left\{w\right\} - \Omega^2 \left[I\right] \left[m\right] \left[y\right] \left\{w\right\} \qquad \text{(A-20)}$$

$$- \Omega^2 \left[I\right] \left[S_\alpha\right] \left[y\right] \left\{\alpha\right\} - \omega^2 \left[I\right]^2 \left[m\right] \left\{w\right\}$$

$$- \omega^2 \left[I\right] \left[S_\alpha\right] \left\{\alpha\right\} + \left[I\right] \left\{K_1\right\} + \left\{K_2\right\} = \left\{0\right\}$$

Equation (A-20) may be premultiplied by the inverse of the bending stiffness matrix $\left[EI\right]$ and then integrated twice. The result after each of the successive integrations is given by the following equations:

$$\{w'\} - [I][EI]^{-1}[T]\{w\} - \Omega^2[I][EI]^{-1}[I][m][y]\{w\} \qquad \text{(A-21)}$$

$$- \Omega^2[I][EI]^{-1}[I][S_\alpha][y]\{\alpha\} - \omega^2[I][EI]^{-1}[I]^2[m]\{w\}$$

$$- \omega^2[I][EI]^{-1}[I]^2[S_\alpha]\{\alpha\} + [I][EI]^{-1}[I]\{K_1\}$$

$$+ [I][EI]^{-1}\{K_2\} + \{K_3\} = \{0\}$$

$$\{w\} - [I]^2[EI]^{-1}[T]\{w\} - \Omega^2[I]^2[EI]^{-1}[I][m][y]\{w\} \qquad \text{(A-22)}$$

$$- \Omega^2[I]^2[EI]^{-1}[I][S_\alpha][y]\{\alpha\} - \omega^2[I]^2[EI]^{-1}[I]^2[m]\{w\}$$

$$- \omega^2[I]^2[EI]^{-1}[I]^2[S_\alpha]\{\alpha\} + [I]^2[EI]^{-1}[I]\{K_1\}$$

$$+ [I]^2[EI]^{-1}\{K_2\} + [I]\{K_3\} + \{K_4\} = \{0\}$$

In order to evaluate the constant of integration matrices in Equation (A-22) cantilever-free boundary conditions are assumed. These boundary conditions are

$$(w)_o = 0 \qquad \text{(A-23)}$$

$$(w')_o = 0 \qquad \text{(A-24)}$$

$$\left(EIw''\right)_n = 0 \tag{A-25}$$

$$\left(EIw''\right)_n' - \left(Tw'\right)_n - \Omega^2 \left(S_{\alpha y}\alpha\right)_n = 0 \tag{A-26}$$

$$\left(T\right)_n = 0 \tag{A-27}$$

where the subscripts o and n indicate that the associated quantity is at the root $\left(y = y_o\right)$ or at the tip $\left(y = y_n\right)$.

In order to extract the appropriate conditions at $y = y_o$ and $y = y_n$ from the preceding relations, the following operator matrices are introduced.

$$\left[L_o\right] = \begin{bmatrix} 1 & 0 & \cdots & 0 \\ 1 & 0 & \cdots & 0 \\ \vdots & \vdots & & \vdots \\ 1 & 0 & \cdots & 0 \end{bmatrix} \tag{A-28a}$$

$$\left[L_n\right] = \begin{bmatrix} 0 & \cdots & 0 & 1 \\ 0 & \cdots & 0 & 1 \\ \vdots & & \vdots & \vdots \\ 0 & \cdots & 0 & 1 \end{bmatrix} \tag{A-28b}$$

The constant of integration matrix $\{K_1\}$ is evaluated by premultiplying Equation (A-17) by $[L_n]$ and applying the boundary condition given by Equation (A-26). Since $[L_n]\{K_1\} = \{K_1\}$, the premultiplication gives

$$\{K_1\} = \omega^2 [L_n][I][m]\{w\} + \omega^2 [L_n][I][S_\alpha]\{\alpha\} \qquad \text{(A-29)}$$

Substituting Equation (A-29) for $\{K_1\}$ into Equation (A-20), premultiplying by $[L_n]$, and applying the boundary conditions of Equations (A-25) and (A-27) yields

$$\{K_2\} = \Omega^2 [L_n][I][m][y]\{w\} + \Omega^2 [L_n][I][S_\alpha][y]\{\alpha\} \qquad \text{(A-30)}$$

$$+ \omega^2 [L_n][I]^2[m]\{w\} + \omega^2 [L_n][I]^2[S_\alpha]\{\alpha\}$$

$$- \omega^2 [L_n][I][L_n][I][m]\{w\} - \omega^2 [L_n][I][L_n][I][S_\alpha]\{\alpha\}$$

Premultiplying Equation (A-21) by $[L_o]$ and applying the boundary condition given by Equation (A-24) yields

$$\{K_3\} = \{0\} \qquad \text{(A-31)}$$

Similary, the premultiplication of Equation (A-22) by $[L_o]$ and applying the boundary condition given by Equation (A-23) yields

$$\{K_4\} = \{0\} \tag{A-32}$$

Substituting Equations (A-29), (A-30), (A-31) and (A-32) into Equation (A-22) yields

$$\{w\} - [I]^2 [EI]^{-1} [T] \{w\} - \Omega^2 [I]^2 [EI]^{-1} [I] [m] [y] \{w\} \tag{A-33}$$

$$- \Omega^2 [I]^2 [EI]^{-1} [I] [S_\alpha] [y] \{\alpha\} - \omega^2 [I]^2 [EI]^{-1} [I]^2 [m] \{w\}$$

$$- \omega^2 [I]^2 [EI]^{-1} [I]^2 [S_\alpha] \{\alpha\} + \omega^2 [I]^2 [EI]^{-1} [I] [L_n] [I] [m] \{w\}$$

$$+ \omega^2 [I]^2 [EI]^{-1} [I] [L_n] [I] [S_\alpha] \{\alpha\} + \Omega^2 [I]^2 [EI]^{-1} [L_n] [I] [m] [y] \{w\}$$

$$+ \Omega^2 [I]^2 [EI]^{-1} [L_n] [I] [S_\alpha] [y] \{\alpha\} + \omega^2 [I]^2 [EI]^{-1} [L_n] [I]^2 [m] \{w\}$$

$$+ \omega^2 [I]^2 [EI]^{-1} [L_n] [I]^2 [S_\alpha] \{\alpha\} - \omega^2 [I]^2 [EI]^{-1} [L_n] [I] [L_n] [I] [m] \{w\}$$

$$- \omega^2 [I]^2 [EI]^{-1} [L_n] [I] [L_n] [I] [S_\alpha] \{\alpha\} = \{0\}$$

A relation for the axial force T may be obtained from Equation (A-14). Integrating this equation numerically gives

$$\{T\} + \Omega^2 [I] [m] [y] \{1\} + \{K_5\} = \{0\} \tag{A-34}$$

Premultiplying Equation (A-34) by $[L_n]$ and applying the boundary condition of Equation (A-27) gives

$$\{K_5\} = -\Omega^2 [L_n] [I] [m] [y] \{1\} \tag{A-35}$$

If the matrix $[F]$ is defined as

$$[F] = [[L_n] - [1]] [I] \tag{A-36}$$

then Equation (A-34) may be expressed by

$$\{T\} = \Omega^2 [F] [m] [y] \{1\} \tag{A-37}$$

Equation (A-33) requires that the axial force matrix $[T]$ be a diagonal matrix; however, Equation (A-37) is a column matrix. To transfer the elements T_i of the column matrix to a diagonal matrix, let $[Q]$ be a diagonal matrix whose diagonal elements are the same as the elements of the corresponding row elements of the column matrix $[F] [m] [y] \{1\}$. Thus,

$$\left[T\right] = \Omega^2 \left[Q\right] \tag{A-38}$$

where

$$\left[Q\right] = \text{diag}\left[F\right]\left[m\right]\left[y\right]\{1\} \tag{A-39}$$

Substituting Equation (A-38) into Equation (A-33) and using Equation (A-36) to combine terms yields

$$\{w\} + \Omega^2 \left[I\right]^2 \left[EI\right]^{-1} \left[F\right]\left[m\right]\left[y\right]\{w\} \tag{A-40}$$

$$+ \Omega^2 \left[I\right]^2 \left[EI\right]^{-1} \left[F\right]\left[S_\alpha\right]\left[y\right]\{\alpha\}$$

$$- \Omega^2 \left[I\right]^2 \left[EI\right]^{-1} \left[Q\right]\{w\}$$

$$- \omega^2 \left[I\right]^2 \left[EI\right]^{-1} \left[F\right]^2 \left[m\right]\{w\}$$

$$- \omega^2 \left[I\right]^2 \left[EI\right]^{-1} \left[F\right]^2 \left[S_\alpha\right]\{\alpha\} = \{0\}$$

Equation (A-13) may be written in matrix form as

$$\left\{ \left(\left[GJ \right] \left\{ \alpha' \right\} \right)' \right\} - \Omega^2 \left[S_\alpha \right] \left[y \right] \left[D \right] \left\{ w \right\} \qquad \text{(A-41)}$$

$$- \Omega^2 \left[I_1 - I_2 \right] \left\{ \alpha \right\} + \omega^2 \left[S_\alpha \right] \left\{ w \right\}$$

$$+ \omega^2 \left[I_\alpha \right] \left\{ \alpha \right\} = \left\{ 0 \right\}$$

The matrix $\left[D \right]$ is a differentiating matrix obtained from Newton's forward-difference interpolation formula of the fourth order given by

$$f(y) = g(s)$$

$$= f_0$$

$$+ \frac{1}{1!} \, s \, \Delta^1 f_0$$

$$+ \frac{1}{2!} \, s(s - 1) \, \Delta^2 f_0$$

$$+ \frac{1}{3!} \, s(s - 1) \, (s - 2) \, \Delta^3 f_0$$

$$+ \frac{1}{4!} \, s(s - 1) \, (s - 2) \, (s - 3) \, \Delta^4 f_0$$

where s and $\Delta^n f_0$ have been defined in the development of the integrating matrix. Expansion of the difference formula becomes

$$g(s) = f_0$$

$$+ \left(f_1 - f_0\right)$$

$$+ \frac{1}{2}\left(s^2 - s\right)\left(f_2 - 2f_1 + f_0\right)$$

$$+ \frac{1}{6}\left(s^3 - 3s^2 + 2s\right)\left(f_3 - 3f_2 + 3f_1 - f_0\right)$$

$$+ \frac{1}{24}\left(s^4 - 6s^3 + 11s^2 - 6s\right)\left(f_4 - 4f_3 + 6f_2 - 4f_1 + f_0\right)$$

Differentiation of this function with respect to s yields the desired approximate derivative of $f(y)$ as

$$\frac{df(y)}{dy} = \frac{1}{P}\,\frac{dg(s)}{ds}$$

and the resulting differentiating matrix as

$$\left[D\right] = \frac{1}{12P}\begin{bmatrix} -25 & 48 & -36 & 16 & -3 & 0 & \cdots & 0 \\ -3 & -10 & 18 & -6 & 1 & 0 & \cdots & 0 \\ 1 & -8 & 0 & 8 & -1 & 0 & & \\ 0 & & & & & & & \\ & & & & & & & 0 \\ & & & 0 & 1 & -8 & 0 & 8 & -1 \\ 0 & \cdots & 0 & -1 & 6 & -18 & 10 & 3 \\ 0 & \cdots & 0 & 3 & -16 & 36 & -48 & 25 \end{bmatrix}$$

Equation (A-41) can be numerically integrated by premultiplying by the integrating matrix $\left[I\right]$ to give

$$\left[GJ\right]\left\{\alpha'\right\} - \Omega^2\left[I\right]\left[S_\alpha\right]\left[y\right]\left[D\right]\left\{w\right\} \qquad \text{(A-42)}$$

$$- \Omega^2\left[I\right]\left[I_1 - I_2\right]\left\{\alpha\right\} + \omega^2\left[I\right]\left[S_\alpha\right]\left\{w\right\}$$

$$- \omega^2\left[I\right]\left[I_\alpha\right]\left\{\alpha\right\} + \left\{K_6\right\} = \left\{0\right\}$$

Premultiplying Equation (A-42) by the inverse of the torsional stiffness matrix $\left[GJ\right]$ and again integrating numerically with $\left[I\right]$ yields

$$\{\alpha\} - \Omega^2 \left[I\right]\left[GJ\right]^{-1}\left[I\right]\left[S_\alpha\right]\left[y\right]\left[D\right]\{w\} \qquad \text{(A-43)}$$

$$- \Omega^2 \left[I\right]\left[GJ\right]^{-1}\left[I\right]\left[I_1 - I_2\right]\{\alpha\}$$

$$+ \omega^2 \left[I\right]\left[GJ\right]^{-1}\left[I\right]\left[S_\alpha\right]\{w\}$$

$$+ \omega^2 \left[I\right]\left[GJ\right]^{-1}\left[I\right]\left[I_\alpha\right]\{\alpha\}$$

$$+ \left[I\right]\left[GJ\right]^{-1}\{K_6\} + \{K_7\} = \{0\}$$

The constant of integration matrices $\{K_6\}$ and $\{K_7\}$ can be evaluated by applying the following boundary conditions for the cantilever-free rotor.

$$\left(\alpha\right)_o = 0 \qquad \text{(A-44)}$$

$$\left(GJ\alpha'\right)_n = 0 \qquad \text{(A-45)}$$

These conditions can be written in matrix form as

$$\left[L_o\right]\left\{\alpha\right\} = \left\{0\right\} \tag{A-46}$$

$$\left[L_n\right]\left[GJ\right]\left\{\alpha'\right\} = \left\{0\right\} \tag{A-47}$$

Premultiplying Equation (A-42) by $\left[L_n\right]$ and applying Equation (A-47) yields

$$\left\{K_6\right\} = \Omega^2\left[L_n\right]\left[I\right]\left[S_\alpha\right]\left[y\right]\left[D\right]\left\{w\right\} \tag{A-48}$$

$$+ \Omega^2\left[L_n\right]\left[I\right]\left[I_1 - I_2\right]\left\{\alpha\right\}$$

$$- \omega^2\left[L_n\right]\left[I\right]\left[S_\alpha\right]\left\{w\right\}$$

$$- \omega^2\left[L_n\right]\left[I\right]\left[I_\alpha\right]\left\{\alpha\right\}$$

Premultiplying Equation (A-43) by $\left[L_o\right]$ and applying the boundary condition given by Equation (A-46) gives

$$\left\{K_7\right\} = \left\{0\right\} \tag{A-49}$$

Substituting Equations (A-48) and (A-49) into (A-43) yields

$$\{\alpha\} - \Omega^2 \left[I\right] \left[GJ\right]^{-1} \left[I\right] \left[S_\alpha\right] \left[y\right] \left[D\right] \{w\} \qquad \text{(A-50)}$$

$$- \Omega^2 \left[I\right] \left[GJ\right]^{-1} \left[I\right] \left[I_1 - I_2\right] \{\alpha\}$$

$$+ \omega^2 \left[I\right] \left[GJ\right]^{-1} \left[I\right] \left[S_\alpha\right] \{w\}$$

$$+ \omega^2 \left[I\right] \left[GJ\right]^{-1} \left[I\right] \left[I_\alpha\right] \{\alpha\}$$

$$+ \Omega^2 \left[I\right] \left[GJ\right]^{-1} \left[L_n\right] \left[I\right] \left[S_\alpha\right] \left[y\right] \left[D\right] \{w\}$$

$$+ \Omega^2 \left[I\right] \left[GJ\right]^{-1} \left[L_n\right] \left[I\right] \left[I_1 - I_2\right] \{\alpha\}$$

$$- \omega^2 \left[I\right] \left[GJ\right]^{-1} \left[L_n\right] \left[I\right] \left[S_\alpha\right] \{w\}$$

$$- \omega^2 \left[I\right] \left[GJ\right]^{-1} \left[L_n\right] \left[I\right] \left[I_\alpha\right] \{\alpha\} = \{0\}$$

Substituting $\left[F\right]$ defined by Equation (A-36) simplifies this expression to

$$\{\alpha\} + \Omega^2 \left[I\right] \left[GJ\right]^{-1} \left[F\right] \left[S_\alpha\right] \left[y\right] \left[D\right] \{w\} \qquad \text{(A-50a)}$$

$$+ \Omega^2 \left[I\right] \left[GJ\right]^{-1} \left[F\right] \left[I_1 - I_2\right] \{\alpha\}$$

$$- \omega^2 \left[I\right] \left[GJ\right]^{-1} \left[F\right] \left[S_\alpha\right] \{w\}$$

$$- \omega^2 \left[I\right] \left[GJ\right]^{-1} \left[F\right] \left[I_\alpha\right] \{\alpha\} = \{0\}$$

Combining the coefficients of $\{w\}$ and $\{\alpha\}$ in Equations (A-40) and (A-50a) while keeping the ω^2 terms separate yields

$$\left[\left[1\right] + \Omega^2 \left[I\right]^2 \left[EI\right]^{-1} \left[\left[F\right] \left[m\right] \left[y\right] - \left[Q\right] \right] \right] \{w\} \qquad \text{(A-51)}$$

$$+ \Omega^2 \left[I\right]^2 \left[EI\right]^{-1} \left[F\right] \left[S_\alpha\right] \left[y\right] \{\alpha\}$$

$$= \omega^2 \left[I\right]^2 \left[EI\right]^{-1} \left[F\right]^2 \left[m\right] \{w\}$$

$$+ \omega^2 \left[I\right]^2 \left[EI\right]^{-1} \left[F\right]^2 \left[S_\alpha\right] \{\alpha\}$$

$$\Omega^2 \left[I\right] \left[GJ\right]^{-1} \left[F\right] \left[S_\alpha\right] \left[y\right] \left[D\right] \left\{w\right\} \tag{A-52}$$

$$+ \left[\left[1\right] + \Omega^2 \left[I\right] \left[GJ\right]^{-1} \left[F\right] \left[I_1 - I_2\right] \right] \left\{\alpha\right\}$$

$$= \omega^2 \left[I\right] \left[GJ\right]^{-1} \left[F\right] \left[S_\alpha\right] \left\{w\right\}$$

$$+ \omega^2 \left[I\right] \left[GJ\right]^{-1} \left[F\right] \left[I_\alpha\right] \left\{\alpha\right\}$$

Equations (A-51) and (A-52) can be combined into a single partitioned matrix equation as

$$\omega^2 \left[A\right] \left\{\phi\right\} = \left[B\right] \left\{\phi\right\} \tag{A-53}$$

where

$$\left\{\phi\right\} = \begin{Bmatrix} \{w\} \\ - - \\ \{\alpha\} \end{Bmatrix}$$

$$\left[A\right] = \left[\begin{array}{c|c} \left[I\right]^2 \left[EI\right]^{-1} \left[F\right]^2 \left[m\right] & \left[I\right]^2 \left[EI\right]^{-1} \left[F\right]^2 \left[S_\alpha\right] \\ \hline \left[I\right] \left[GJ\right]^{-1} \left[F\right] \left[S_\alpha\right] & \left[I\right] \left[GJ\right]^{-1} \left[F\right] \left[I_\alpha\right] \end{array}\right]$$

$$
\left[B\right] = \left[\begin{array}{l|l}
\left[1\right] + & \Omega^2 \left[I\right]^2 \left[EI\right]^{-1} \left[F\right] \left[S_\alpha\right] \left[y\right] \\
\Omega^2 \left[I\right]^2 \left[EI\right]^{-1} \left[\left[F\right] \left[m\right] \left[y\right] - \left[Q\right]\right] & \\
\hline
\Omega^2 \left[I\right] \left[GJ\right]^{-1} \left[F\right] \left[S_\alpha\right] \left[y\right] \left[D\right] & \left[1\right] + \\
 & \Omega^2 \left[I\right] \left[GJ\right]^{-1} \left[F\right] \left[I_1 - I_2\right]
\end{array}\right]
$$

The eigenvalue problem defined by Equation (A-53) can be written in a more familiar form by defining a dynamic matrix, $\left[\bar{C}\right]$, as

$$\left[\bar{C}\right] = \left[B\right]^{-1} \left[A\right]$$

to yield

$$\left[\bar{C}\right] \left\{\phi\right\} = \frac{1}{\omega^2} \left\{\phi\right\}$$

which can be solved by many available techniques.

LITERATURE CITED

1. Mendelson, A., "Effect of Centrifugal Force on the Flutter of Uniform Cantilever Beams at Subsonic Speeds with Application to Compressor and Turbine Blades," NACA Technical Note 1893, 1949.

2. Rosenberg, R., "Aero-Elastic Instability in Unbalanced Lifting Rotor Blades," Journal of the Aerospace Sciences, October, 1944.

3. Gerstenberger, W., and Wood, E. R., "Analysis of Helicopter Aeroelastic Characteristics in High-Speed Flight," American Institute of Aeronautics and Astronautics Journal, Vol. 1, October, 1963.

4. Bisplinghoff, R. L., Ashley, H., and Halfman, R. L., "Aeroelasticity," Addison-Wesley Publishing Company, Inc., Cambridge, Massachusetts, 1955.

5. Turner, M. J., and Duke, J. B., "Propeller Flutter," Journal of the Aerospace Science, Vol. 16, June, 1949.

6. Astill, C. J., and Niebanck, C. F., "Prediction of Rotor Instability at High Forward Speeds," U. S. Army Aviation Material Laboratories, USAAVLABS Technical Report 68-18B, Vol. II, February, 1969.

7. Loewy, R. G., "A Two Dimensional Approximation to the Unsteady Aerodynamics of Rotary Wings," Journal of the Aerospace Sciences, Vol. 24, February, 1957.

8. Jones, J. P., "The Influence of the Wake on the Flutter and Vibration of Rotor Blades," Aeronautical Quarterly, Vol. IX, 1958.

9. Timman, R., and Van de Vooren, A. I., "Flutter of a Helicopter Rotor Rotating in Its Own Wake," Journal of the Aerospace Sciences, Vol. 24, September, 1957.

10. Theodorsen, T., "General Theory of Aerodynamic Instability and the Mechanism of Flutter," NACA TR 496, 1949.

11. Hammond, C. E., "A Parametric Study of Helicopter Rotor Blade Flutter Under Low Inflow Conditions, Using Incompressible Aerodynamics," Georgia Institute of Technology, School of Aerospace Engineering, A.E. 604 Special Problem, June 1968.

12. Ham, N. D., Moser, H. H., and Zvara, J., "Investigation of Rotor Response to Vibratory Aerodynamic Inputs, Part I. Experimental Results and Correlation with Theory," U. S. Air Force, Air Research and Development Command, WADC TR 58-87, AD 203389, October 1958.

13. Miller, R. H., "Theoretical Determination of Rotor Blade Harmonic Airloads," Massachusetts Institute of Technology, Aeroelastic and Structures Research Laboratory, TR 107-2, AD-619048, August 1964.

14. Ashley, H., Moser, H. H., and Dugundji, J., "Investigation of Rotor Response to Vibratory Aerodynamic Inputs," Part III. "Three-Dimensional Effects on Unsteady Flow Through A Helicopter Rotor," U. S. Air Force, Air Research and Development Command, WADC TR 58-87, AD 203392, October 1958.

15. Reissner, E., "Effect of Finite Span on the Airload Distributions for Oscillating Wings - I: Aerodynamic Theory of Oscillating Wings of Finite Span," NACA TN 1194, March 1947.

16. Ichikawa, T., "Linear Aerodynamic Theory of Rotor Blades," Journal of Aircraft, Vol. 4, No. 3, May-June 1967, pp 210-218.

17. Weissinger, J., "The Lift Distribution of Swept-Back Wings," NACA TM 1120, 1947.

18. Jones, W. P., and Rao, B. M., "Compressibility Effect on Oscillating Rotor Blades in Hovering Flight," American Institute of Aeronautics and Astronautics Journal, February 1970.

19. Jones, W. P., "The Oscillating Airfoil in Subsonic Flow," British Aeronautical Research Council, R & M 2921, 1956.

20. Hammond, C. E., "Compressibility Effects in Helicopter Rotor Blade Flutter," Georgia Institute of Technology, GITAER 69-4, December 1969.

21. Smilg, B., and Wasserman, L. S., "Application of Three-Dimensional Flutter to Aircraft Structures," Air Force Technical Report 4798, ATI-28690, 1942.

22. Yntema, R. T., "Simplified Procedures and Charts for the Rapid Estimation of Bending Frequencies of Rotating Beams," NACA Technical Note 3459, 1955.

23. Hunter, W. F., "Integrating Matrix Method for Determining the Natural Vibration Characteristics of Propeller Blades," NASA Technical Note D-6064, 1970.

24. Pennington, R. H., Introductory Computer Methods and Numerical Analysis, The Macmillan Company, New York, New York, 1965.

25. Gessow, A., and Myers, Jr., G. C., Aerodynamics of the Helicopter, Frederick Ungar Publishing Co., New York, New York, 1967.

26. Brooks, G. N., and Baker, J. E., "An Experimental Investigation of the Effect of Various Parameters Including Tip Mach Number on the Flutter of Some Helicopter Rotor Models," NACA Technical Note 4005, 1958.

27. Vakhitov, M. B., "Calculation of Free, Joint Bend-Twist Oscillations of Revolving Helicopter Blade," News of Institutions of Higher Learning, Aeronautical Engineering, No. 4, 1963, Collection of Articles (U.S. Air Force Systems Command), AD-629441.

28. Houbolt, J. C., and Brooks, G. W., "Differential Equations of Motion for Combined Flapwise Bending, Chordwise Bending, and Torsion of Twisted Nonuniform Rotor Blades," NACA Technical Report 1346, 1958.

VITA

William Felton White, Jr. was born June 15, 1939, the son of William F. and Rita S. White. After attending elementary schools in Warner Robins, Georgia and Perry, Georgia, he was graduated from Perry High School in June, 1958. He entered Middle Georgia College, Cochran, Georgia in the fall of that year, and in June, 1960 obtained a Diploma of Engineering. He entered Auburn University in September, 1960 and completed the requirements for the degree Bachelor of Aerospace Engineering in August 1962 and the degree of Master of Science in Aerospace Engineering in December 1964.

Upon graduation he was employed as an Assistant Professor in the Aerospace Engineering Department of Auburn University, Auburn, Alabama for three years. He was employed by Boeing Airplane Company, Seattle, Washington for one year prior to entering the Graduate Division of the Georgia Institute of Technology, Atlanta, Georgia. He is a member of Phi Kappa Phi, Tau Beta Pi and Pi Tau Sigma.